Tetrahedron 81 (2021) 131827

Contents lists available at ScienceDirect

Tetrahedron

journal homepage: www.elsevier.com/locate/tet

Synthesis of aminal-type Lilium candidum alkaloids and lilaline; determination of their relative configuration by the concerted use of NMR spectroscopy and DFT conformational analysis

Sándor Nagy [a, 1], Áron Szigetvári [b, 1], Viktor Ilkei [a, c, *], Balázs Krámos [b], Zoltán Béni [b], Csaba Szántay Jr. [b], László Hazai [a]

[a] Department of Organic Chemistry and Technology, Budapest University of Technology and Economics, Budafoki út 8, Budapest, H-1111, Hungary
[b] Spectroscopic Research Department, Gedeon Richter Plc., Gyömrői út 19-21, Budapest, H-1103, Hungary
[c] Medicinal Chemistry Laboratory I, Gedeon Richter Plc., Gyömrői út 19-21, Budapest, H-1103, Hungary

ARTICLE INFO

Article history:
Received 16 September 2020
Received in revised form
27 November 2020
Accepted 29 November 2020
Available online 6 December 2020

Keywords:
Iminium chemistry
Synthesis of lily alkaloids
Determination of relative configuration
Conformational analysis
$^{1}H-^{1}H$ distance measurements by NMR

ABSTRACT

We hereby report the synthesis of six racemic alkaloids isolated from Lilium candidum L. Their common structural feature is a five-membered lactam ring which is, in the case of the flavonoid alkaloid lilaline, attached to the molecule's aromatic core, while in the case of the other five compounds, it is connected to the nitrogen atom of a pyrrolinone ring by an aminal function. The syntheses of these natural products were achieved via Mannich-type alkylations through cyclic N-acyliminium ions as intermediates. Besides the synthesis, the so far unexplored stereochemistry of these natural products was determined by a combination of NMR-based proton−proton distance measurements and theoretical conformational analyses carried out at the DFT level.

1. Introduction

Lilium candidum L. − commonly known as the *Madonna lily* − is a perennial plant in the true lily family. It has a high-growing leafy stem and it bears white, strongly fragrant flowers in the summer. The *Madonna lily* is native to the Balkans and to the Middle East, but it has also become naturalized in other parts of the world [1]. In folk medicine the extract of the plant is used for the treatment of burns, ulcers, inflammation and for healing wounds [2].

Several interesting heterocyclic compounds have been isolated from *Lilium candidum* L. (Fig. 1). Structurally, the largest subclass of the isolated lily alkaloids contains an aminal function or a 3-pyrrolin-2-one moiety (Fig. 1, highlighted in blue). Despite their biological relevance, most members of this special family of lily alkaloids have not yet been synthesized.

Jatropham (**1**) was first isolated from *Jatropha macrorhiza* by Wiedhopf and co-workers [3]. Their initial structural conclusion (the 4-Me analogue of **1** was postulated by the authors) was later revised by Yakushijin et al. [4] and was further verified by two distinct syntheses [5,6]. Jatropham (**1**) was found to show anticarcinogenic [3,7] and cell protecting [8] activity. Methyljatropham (**2**) and ethyljatropham (**3**) were isolated as racemates from *Lilium hansonii* [9] and from *Lilium candidum* [10], respectively. However, the natural origin of these compounds is questionable since their isolation involved extractions by the appropriate alcohols, methanol or ethanol.

Continuing the phytochemical characterization of *Lilium candidum,* Haladová and co-workers later isolated the pyrroline-pyrrolidine alkaloids **4**, **5** and **7** [11], the *N*-pyrrolidonyl derivative of jatropham, **6** [12], and the jatropham dimers **8** and **10** [13]. Although most of these compounds contain two stereogenic centers, neither the isomeric composition, nor the stereochemistry of the isolated products was discussed in these papers. Our literature survey showed that the stereochemistry was only explored in the case of compound **5**, where an (*R*,*R*) relative configuration was suggested on the basis of X-ray analysis [14]. No synthesis of these dimeric pyrroline-alkaloids has been published so far, with the

* Corresponding author. Medicinal Chemistry Laboratory I, Gedeon Richter Plc., Gyömrői út 19-21, Budapest, H-1103, Hungary.
E-mail address: viktor.ilkei@gmail.com (V. Ilkei).
[1] These authors contributed equally.

https://doi.org/10.1016/j.tet.2020.131827

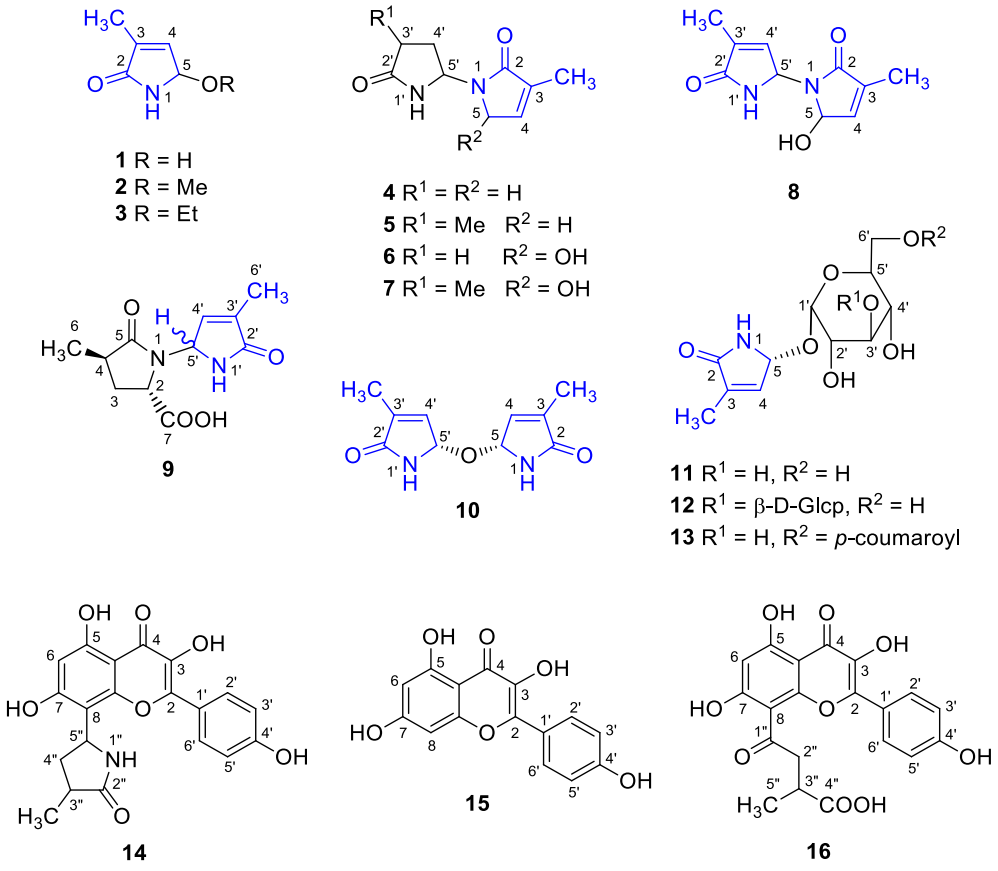

Fig. 1. Pyrroline alkaloids and flavonoid constituents isolated from *Lilium candidum* L. (3-pyrrolin-2-one moieties are highlighted in blue).

exception of jatropham dimer **8**, whose formation was observed by Yakushijin et al. upon the acid treatment of an N-protected derivative of **1** [5].

In addition, the 4-methylpyroglutamic acid derivative of jatropham (**9**) [15] and jatropham glycosides **11** [9], **12** [15] and **13** [16] were isolated from *Lilium hansonii, Lilium martagon* and other related lily species that belong to this structural class.

The flavonoid alkaloid lilaline (**14**), together with its flavonoid core, kaempferol (**15**) and its methylsuccinyl derivative **16** (most probably the biogenetic precursor of **14**), were also isolated from *Lilium candidum* [17–19]. The stereochemistry of **14** has not been clarified in the literature either.

Continuing our investigations in the field of natural product synthesis through iminium chemistry [20], we endeavored to synthesize some of these interesting heterocyclic compounds, focusing primarily on the pyrroline–pyrrolidine type dimers (**4**–**8**) and the flavonoid alkaloid lilaline (**14**). In addition, the so far undetermined stereochemistry of compounds **6**–**8** and **14** prompted us to explore at least their relative configurations using NMR spectroscopy complemented by molecular modeling.

The synthetic strategy we applied here is similar to the method we recently implemented to effectively introduce a substituted 2-pyrrolidon-5-yl group onto nucleophiles, such as heteroatoms or activated aromatic rings [20]. The method involves the synthesis of the appropriate *N*-acylaminocarbinol derivative, which is then allowed to react with the nucleophile of our choice in a *Mannich*-type alkylation reaction [21]. These reactions usually require acid catalysis in order to enable the *in situ* conversion of the electrophile precursor to an *N*-acyliminium ion that can attack the nucleophile to form the desired compounds. The application of this strategy enabled the efficient synthesis of the targeted lily alkaloids from inexpensive, commercially available starting materials.

2. Results and discussion

The retrosynthetic concept of the targeted compounds is outlined in Scheme 1. Five reactants are required for the synthesis of the six alkaloids, demonstrating the versatility of these building blocks in the synthesis of lily alkaloids. The building blocks are 3-methyl-3-pyrrolin-2-one (**17**), 5-ethoxypyrrolidin-2-one (**18**), 5-hydroxy-3-methylpyrrolidin-2-one (**19**), (±)-jatropham [5-hydroxy-3-methyl-3-pyrrolin-2-one] (**1**) and the flavonoid kaempferol (**15**) (Scheme 1), which is the only building block available at a reasonable price.

The synthesis of the four pyrroline and pyrrolidine building blocks was achieved in a few steps from cheap and easily accessible starting materials. 3-Methyl-3-pyrrolin-2-one (**17**) was synthesized in 4 steps from pyrrole (Scheme 2). In the first step the nitrogen atom of pyrrole (**20**) was silylated with the bulky triisopropylsilyl (TIPS) group to yield TIPS-pyrrole (**21**) [23]. This enabled formylation in the subsequent *Vilsmeier reaction* in the C3 position [23,24]. The work-up resulted in desilylation, yielding pyrrole-3-carboxaldehyde (**22**), which was then converted to 3-methylpyrrole (**23**) in a *Wolff-Kishner reduction* [25]. Finally, oxidation of **23** b y aqueous hydrogen peroxide [26] gave the desired lactam **17** in medium yield.

5-Ethoxypyrrolidin-2-one (**18**) was synthesized in a single step from succinimide (**24**) via partial reduction by sodium borohydride and a subsequent one-pot etherification under acidic conditions (Scheme 3), following the procedure described earlier [22,20d].

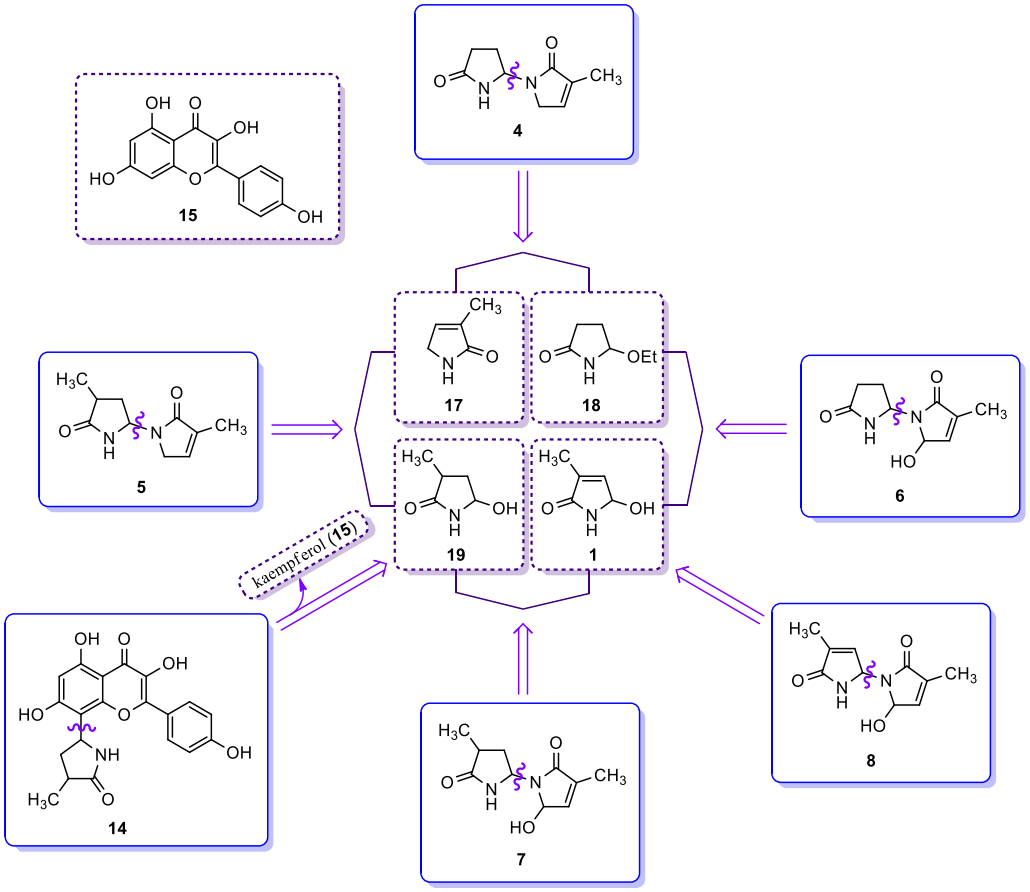

Scheme 1. Retrosynthetic concept of target compounds **4**–**8** and **14**.

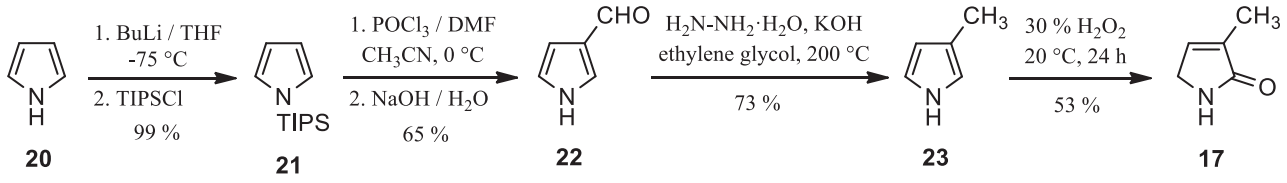

Scheme 2. Synthesis of 3-methyl-3-pyrrolin-2-one (**17**).

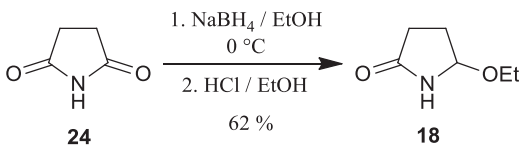

Scheme 3. Synthesis of 5-ethoxypyrrolidin-2-one (**18**).

The cyclic *N*-acylaminocarbinol reagents **1** and **19** were synthesized from citraconic anhydride (**25**) in 2 and 3 steps, respectively (Scheme 4). Citraconic anhydride (**25**) was first converted to citraconimide (**26**) with hexamethyldisilazane (HMDS) in DMF at 100 °C [27], which was reduced with diisobutyl aluminium hydride (DIBALH) in THF at 0 °C to yield (±)-jatropham (**1**) [28]. The regioselectivity of the reduction was confirmed by NMR data. In the HMBC spectrum the methyl group (1.83 ppm) showed correlation to the C-2 carbonyl group (175.5 ppm) while no correlation was observed with the C-5 aminal carbon (80.0 ppm) proving the structure of **1**. In the case of the synthesis of the saturated *N*-acylaminocarbinol **19**, **26** was first reduced by catalytic hydrogenation to (±)-2-methylsuccinimide (**27**) [29], which was then further reduced with DIBALH at 0 °C to give an inseparable mixture of 5-hydroxy-3-methylpyrrolidin-2-one (**19**) and its 2-hydroxy isomer **28**. In contrast to the DIBALH reduction of **26** under similar conditions, the regioselectivity of the reduction of **27** was much lower, the resulting mixture contained **19** and **28** in an approximate ratio of 2.7:1. The regioisomers were identified based on HMBC data. In the case of **19**, the methyl group showed correlation with the C-2 carbonyl group while no correlation to the C-5 aminal-type carbon atom was observed. In contrast, in compound **28**, the methyl group gave correlation to the C-5 aminal-type carbon atom while no correlation to the C-2 carbonyl group was detected. Despite the presence of significant amounts (ca. 27%) of the isomeric *N*-acylaminocarbinol **28** in the obtained isomeric reagent mixture, it could be utilized in the syntheses of the targeted lily alkaloids.

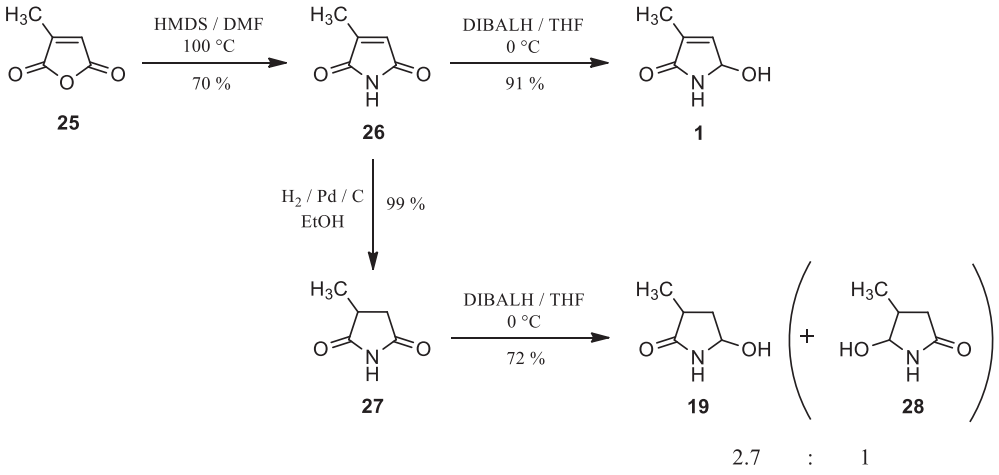

Scheme 4. Synthesis of the cyclic *N*-acylaminocarbinols **1** and **19**.

With the four pyrroline-pyrrolidine building blocks in hand, we synthesized the desired lily alkaloids by the reaction of the two appropriate compounds in THF in the presence of catalytic amounts of *p*-toluenesulfonic acid. The reactants were employed in equimolar amounts and the reactions proceeded to full conversion at room temperature in 1 h. The reactions gave the targeted lily alkaloids **4**–**8** as the major products in medium to high yields (Scheme 5). In the case of the synthesis of **5** and **7** the presence of the isomeric *N*-acylaminocarbinol **28** in the reagent mixture beside the major component **19** was not taken into account, however the reactions still furnished the desired natural products in relatively good yields. The explanation for this observation probably lies in the preferential reaction of the nucleophile with **19** over its isomer **28**, due to the aminal function being present in the sterically more hindered site in the latter compound. And even though one of the multiple minor spots visible beside the major product on the TLC of the rather complex reaction mixtures could possibly belong to a side product arising from **28**, these multicomponent reaction mixtures seemed to contain so many minor and trace products, that no effort was made to isolate and characterize these substances.

In the case of **4** and **8**, the precipitated crystalline products could be isolated by a simple filtration, while in the case of **5** and **6** the products were crystallized after evaporation of the solvent. The pyrroline alkaloid **7** was purified by column chromatography. Compound **4** was isolated as a single racemic compound, while in the case of **5**–**8** due to the presence of multiple stereogenic centers the synthesized lily alkaloids were all isolated as racemic mixtures of diastereomers in different compositions (Scheme 5). These mixtures were subjected to detailed NMR spectroscopic studies.

The mechanism of these aminal-forming *Mannich*-type alkylation reactions involves the *in situ* generation of cyclic *N*-acyliminium ions from their *N*-acylaminocarbinol precursors via protonation of the carbinol oxygen and the subsequent loss of an ethanol (in the case of reagent **18**) or water (in the case of **19** or **1**) molecule. This is followed by the electrophilic attack of the *N*-acyliminium ion on the slightly nucleophilic lactam-nitrogen of the other reactant. This mechanism and the possible side reactions are presented through the example of the synthesis of lily alkaloid **7** (Scheme 6).

The saturated cyclic *N*-acylaminocarbinol **19** is transformed into the *N*-acyliminium ion **29**, which attacks the nitrogen atom of **1**, yielding the desired lily alkaloid **7** as the major product. However, both reactants are *N*-acylaminocarbinol type compounds, thus, theoretically the "reverse alkylation" is possible from the same reactants as well. In this hypothetical side reaction **1** is converted into the *N*-acyliminium ion **30**, which in turn could attack the nitrogen atom of **19**, giving the hypothetical "reverse alkylation" product. Likewise, an *N*-acyliminium ion could also attack the nitrogen atom of its *N*-acylaminocarbinol precursor to yield a "self-alkylation" product. Besides these side reactions, the formation of larger adducts or oligomers composed by one or both reactants in different ratios can be envisaged as well.

Despite these theoretical possibilities, a strong preference for the formation of the expected products was observed in all cases. Considering the formation of **7** as an example (Scheme 6), the reason behind this preference – assuming that both reactive iminium species (**29** and **30**) are present – most probably lies in the reactivities of the similar species, meaning that **29** is a better electrophile than **30** while **1** is a better nucleophile than **19**. Subsequently, the predominant reaction pathway turns out to be the one leading to the formation of **7**, resulting in the desired lily alkaloid as the major product.

Despite the prevalence of the aforementioned reaction route, some of the potentially arising side products could possibly be present in the reaction mixtures. Although in most cases multiple spots were visible on TLC beside the major products, due to the rather complex reaction mixtures, no effort was made to isolate minor or trace products.

The synthesis of lilaline (**14**) was carried out via the reaction of kaempferol (**15**) and a slight excess (1.2 eq.) of **19** at reflux temperature in 2 h in the presence of a catalytic amount of *p*-toluenesulfonic acid and gave the target compound (**14**) in high yield (Scheme 7). Even though the formation of the C6-isomer via C6-amidoalkylation of kaempferol can also be hypothesized based on our previous experience in the field [20c,d], only the C8-isomer (lilaline, **14**) could be isolated from the reaction mixture. This high regioselectivity is in accordance with our earlier finding [20d], showing that phenolic *Mannich reactions* [30] of other 5,7-dihydroxylated flavonoids proceed with high regioselectivity as well. Lilaline (**14**) was purified by preparative HPLC and was obtained as a diastereomeric mixture. The ratio of the major trans diastereomer and the minor cis isomer in the final product was found to be approx. 3:1 (according to the ^{1}H NMR data).

2.1. Determination of the relative configuration of compounds 6, 7 and 8

Firstly, the elemental composition and the constitution of all

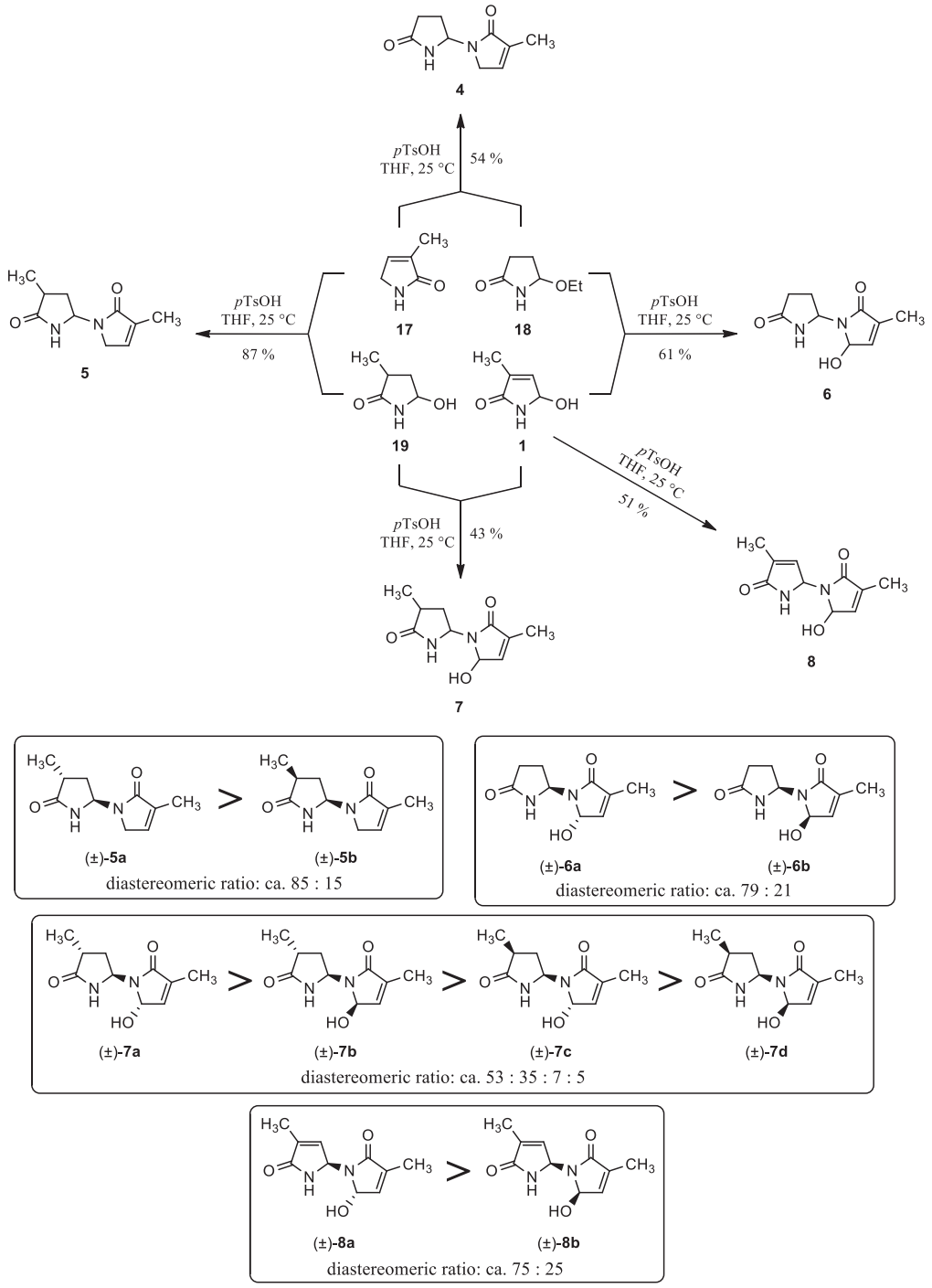

Scheme 5. Synthesis of lily alkaloids **4**–**8** and the diastereomeric composition of the synthesized products.

synthetic products were elucidated using high resolution mass spectrometry and standard NMR spectroscopic methods (^{1}H, ^{13}C NMR, ^{1}H–^{1}H COSY, ^{1}H–^{1}H NOESY or ROESY, ^{1}H–^{13}C HSQC and ^{1}H–^{13}C HMBC). Based on the spectral data complete ^{1}H and ^{13}C NMR characterization of each stereoisomer of the expected products could be achieved. Regarding the stereochemistry, the relative configuration of compounds **5** and **14** could easily be deduced on the basis of Nuclear Overhauser Effect (NOE) data (protons or functional groups that are situated on the same face of a ring are likely to attain spatial proximity; the spatial proximity of protons gives rise to strong peaks in the NOESY spectra, see Fig. 2). For both **5** and **14**, the 3,5-trans isomers were found to be the major products.

Determining the stereochemistry of **6**, **7** and **8** was more challenging, because in these cases the chirality centers in the two rings are connected by a freely rotating C–N bond (Fig. 3).

As is well known, for two protons whose distance varies in time due to a fast conformational motion, the magnitude of the observed ^{1}H–^{1}H NOE is a function of the conformational energy profile of the system [31]. Thus, without knowledge of the pertinent

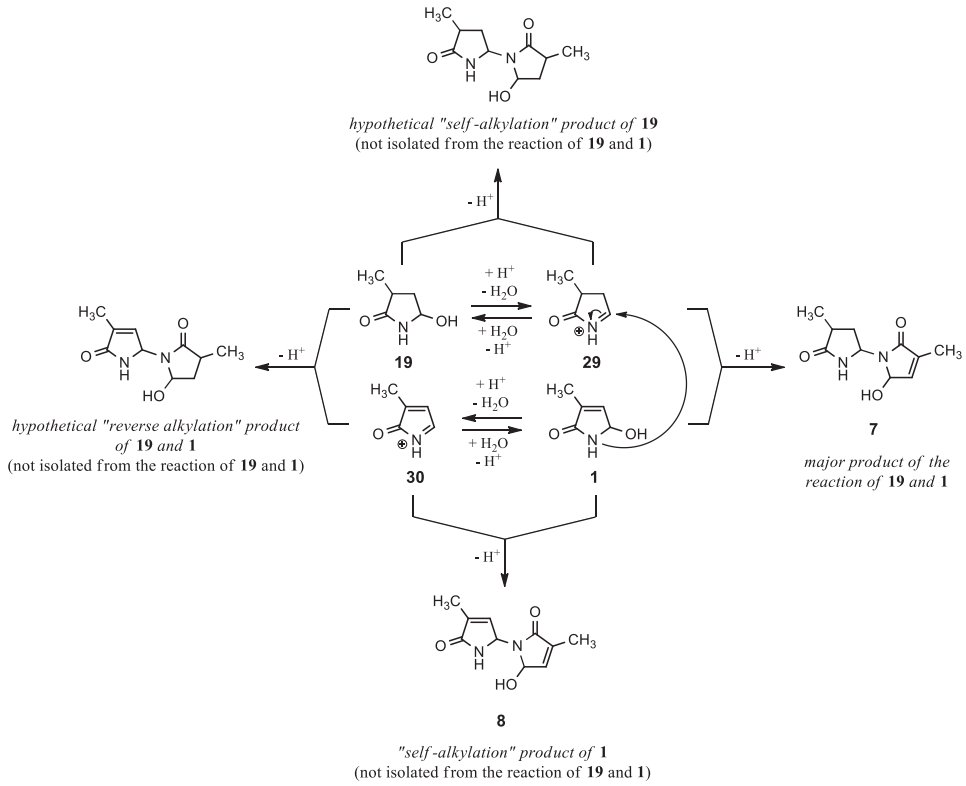

Scheme 6. A plausible mechanism of aminal-forming *Mannich*-type alkylations and the possible side reactions presented through the example of the synthesis of lily alkaloid **7**.

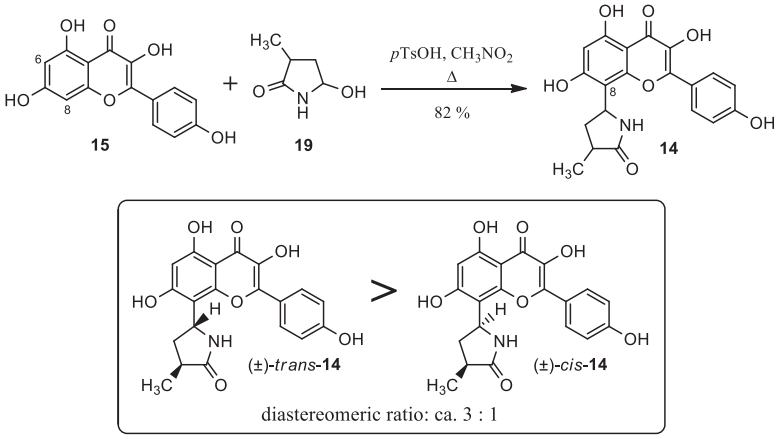

Scheme 7. Synthesis of the flavonoid alkaloid lilaline (**14**).

conformational profiles of the possible configurational isomers of compounds **6**, **7** and **8**, and without knowing that there is a suitably large difference between the profiles associated with the configurational isomers, the relative configurations cannot be determined reliably from the measured $^{1}H-^{1}H$ NOEs. A comparison of the corresponding selective inversion 1D NOESY spectra showed that the different stereoisomers gave rise to the same resonances but with substantially different intensities, which suggested that such a marked configuration-dependent difference in the conformational energy profiles exists, and so the relative configurations can be determined if the NOE measurements are complemented by a molecular modeling study. As shown by literature examples [32–34] the QM-based calculation, followed by a sophisticated statistical analysis of the calculated ^{1}H and ^{13}C NMR chemical shifts with respect to the experimental ones might have been another approach to assign the relative configurations of **6**, **7**, and **8.** However, in these cases larger differences were obtained in the NOE intensities than between the chemical shifts (see SI) of the diastereoisomers. This has prompted us to use the NOE derived distances as reference in our modeling study.

We note in passing that for compound **7** the determination of the relative configuration of C-3′ and C-5’ was straightforward from routine 2D NOESY spectra.

Running selective inversion 1D NOESY experiments with appropriate choice of the experimental parameters (application of low-viscosity solvents, choice of relatively short mixing times

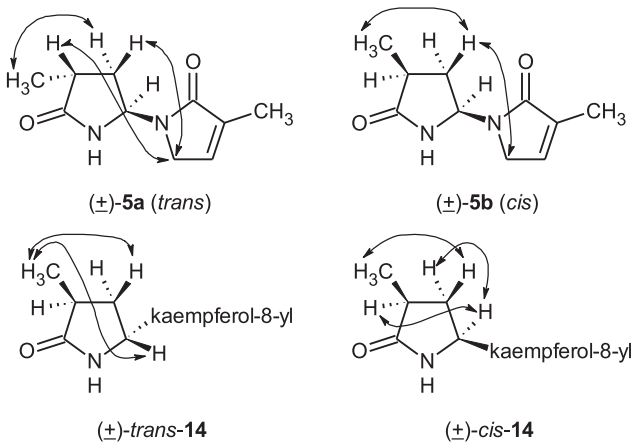

Fig. 2. Diagnostic NOE correlations used to determine the relative configuration of compounds **5** and **14**.

mixture of acetone-d_6 and methanol-d_4 [12], **7**: acetone-d_6 [11], and **8**: methanol-d_4 [13]), since their viscosity (acetone: $3.2 \cdot 10^{-4}$ Pa s, methanol: $5.6 \cdot 10^{-4}$ Pa s at 300 K[37]) was suitable for the NOE measurements. To maximize the signal-to-noise ratio of the 1D NOESY spectra, which was a critical feature when acquiring the spectra of the minor diastereomers, we chose the upper bound of the mixing times (600 ms) that Butts et al. recommended to use [35], since the NOE intensity is proportional to the mixing time in the early section of the NOE buildup curve [31]. From the various pulse sequences known for distance measurements [38], we chose a single pulse field gradient spin-echo, zero-quantum filtered selective inversion 1D NOESY sequence (*selnogpzs.2*), which was part of the spectrometer's standard pulse sequence library.

For the analysis of the stereoisomeric mixtures of the lily alkaloids obtained in the syntheses we took advantage of the large resolving power of our 800 MHz NMR spectrometer, instead of resorting to the separation of these diastereomers (*e.g.* by preparative HPLC). This approach not only saved time and effort but

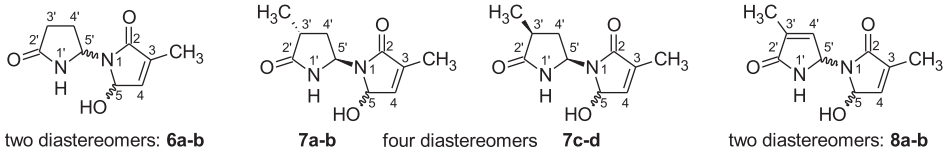

Fig. 3. Stereoisomers of compounds **6**, **7** and **8**.

relative to the T_1 relaxation times) enable us to determine interproton distances with high accuracy. Using the conventional notation, let *S* denote the selectively inverted proton, and let *I* be any other proton in the molecule on which we observe the NOE as a result of having inverted S. According to Butts et al., in such an experiment the NOE at spin *I* is to a very good approximation proportional to the negative sixth power of the distance $d_{I,S}$ [31] between *I* and *S*; the margin of error for the distance measurement is *ca.* 4% [35]. Jones et al. were able to achieve the same margin of error of interproton distance measurements in a flexible molecule (4-propylaniline) that can adopt several well-defined low-energy conformations [36].

For the interproton distance measurements of **6**, **7** and **8**, we used solvents or solvent mixtures that were identical to the ones used by the authors who provided the spectral characterization of the lily alkaloids isolated from natural sources (**6**: equal volume ensured that for all isomers in a sample the 1D NOESY measurements were carried out under exactly the same measurement conditions (pH, temperature, molarity of the components, *etc.*). In this way, any biases in distance measurements due to differences in sample preparation and other experimental conditions could be avoided, which was critical for a reliable comparison of the data.

The measured 1D NOESY intensities are reported in Tables 1–3; the intensities are given relative to that of the selectively inverted (−100%) resonance (in all cases that was the CH(OH) proton at position 5 in the 1-alkyl-3-pyrrolin-2-one ring). The experimental distances were determined by the following equation

$$d_{I,S} = d_{Ref,S} \cdot \left(\frac{\eta_{I,S}}{\eta_{Ref,S}} \right)^{-6}$$

where *I* is the investigated proton, *S* is the selectively inverted

Table 1
Measured NOE intensities and estimated interproton distances in the stereoisomers of **6**.

6a (major isomer)		Relative intensity	Estimated distance	**6b** (minor isomer)		Relative intensity	Estimated distance
Inverted proton	H-5 (δ 5.54)	−100%	–	Inverted proton	H-5 (δ 5.48)	−100%	–
Observed protons	H-4 (δ 6.67)	1.063%	2.69 Å (calib.)	Observed protons	H-4 (δ 6.68)	1.032%	2.69 Å (calib.)
	H-5' (δ 5.51)	0.391%	3.18 Å		H-5' (δ 5.73)	0.340%	3.24 Å
	H^b -4' (δ 2.35)	0.896%	2.77 Å		H^b -4' (δ 2.38)	0.140%	3.75 Å

The ratio of stereoisomers **6a**:**6b** was ca. 79:21.

Table 2
Measured NOE intensities and estimated proton-proton distances in the stereoisomers of **7**.

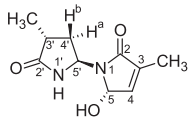

(±)-**7a**

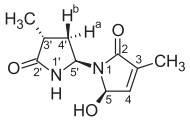

(±)-**7b**

7a (major „trans" isomer)		Relative intensity	Estimated distance	**7b** (minor „trans" isomer)		Relative intensity	Estimated distance
Inverted proton	H-5* (δ 5.57)	−100%	–	Inverted proton	H-5 (δ 5.48)	−100%	–
Observed protons	H-4 (δ 6.63)	0.612%	2.69 Å (calib.)	Observed protons	H-4 (δ 6.64)	0.586%	2.69 Å (calib.)
	H-5' (δ 5.42)	0.324%	2.99 Å		H-5' (δ 5.62)	0.163%	3.33 Å
	H^b -4' (δ 2.54)	0.562%	2.73 Å		H^b -4' (δ 2.56)	0.065%	3.88 Å

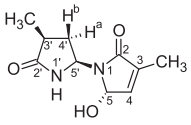

(±)-**7c**

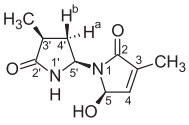

(±)-**7d**

7c (major „cis" isomer)		Relative intensity	Estimated distance	**7d** (minor „cis" isomer)		Relative intensity	Estimated distance
Inverted proton	H-5# (δ ~5.63)	(overlapped)	–	Inverted proton	H-5# (δ ~5.64)	(overlapped)	–
Observed protons	H-4 (δ 6.64)	0.298%	2.69 Å (calib.)	Observed protons	H-4 (δ 6.65)	0.137%	2.69 Å (calib.)
	H-5' (δ 5.54)	0.164%	2.97 Å		H-5' (δ 5.68)	0.040%	3.30 Å
	H^b -4' (δ 2.17)	0.393%	2.57 Å		H^b -4' (δ 2.39)	0.027%	3.53 Å+

"Cis" and "trans" refer to the relative configuration in the pyrroline-2-one ring (C-3′ and C-5′).
The ratio of stereoisomers **7a**:**7b**:**7c**:**7d** was ca. 53:35:7:5.
*Due to overlap of the signals in the ^{1}H NMR spectrum we could not avoid inverting H-5′ of **7c**.
#Due to spectral overlap we could only invert H-5 of **7c**, H-5 of **7d** and H-5′ of **7b** together.
+Since the intensity of the detected NOE signal is close to the detection limit, the error of quantitation might be larger than in the other cases.

Table 3
Measured NOE intensities and estimated proton-proton distances in the stereoisomers of **8**.

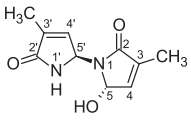

(±)-**8a**

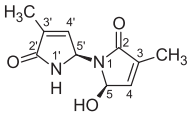

(±)-**8b**

8a (major isomer)		Relative intensity	Estimated distance	**8b** (minor isomer)		Relative intensity	Estimated distance
Inverted proton	H-5 (δ 5.40)	−100%	–	Inverted proton	H-5 (δ 5.25)	−100%	–
Observed protons	H-4 (δ 6.64)	1.187%	2.69 Å (calib.)	Observed protons	H-4 (δ 6.67)	1.172%	2.69 Å (calib.)
	H-5' (δ 5.96)	0.343%	3.31 Å		H-5' (δ 6.11)	0.199%	3.61 Å
	H-4' (δ 6.76)	0.747%	2.91 Å		H-4' (δ 6.78)	0.133%	3.87 Å

The ratio of stereoisomers **8a**:**8b** was ca. 65:35 at the time of the 1D NOESY measurements.

proton, $d_{Ref,S}$ is a reference distance (2.69 Å, calculated for H-5 – H-4 by molecular modeling) for calibration, and η is the measured relative signal intensity in the 1D NOESY spectrum. The decisive interproton distances were H-5 – H-5′ and H-5 – H-4′, i.e. the distances between the protons belonging to different rings.

A comparison of the estimated distances of the stereoisomers showed that in the case of **6** and **7** the H-5 – H^b-4′ distance, while in the case of **8** the H-5 – H-4' distance, is consistently shorter by about 1 Å in the so-called "major" isomers than in the "minor" isomers. One angstrom difference, which corresponds to ca. 30%, is significant and can be used for the stereochemical assignment. In order to interpret these substantial differences in the critical distances theoretical calculations were undertaken.

Firstly, conformational search was performed at the MM (OPLS3) level for all stereoisomers of compounds **6**–**8** (only a single enantiomer, in which the configuration of C-5′ was arbitrarily taken to be *R*, was considered in all cases). The lowest energy conformers (using the default MacroModel setting, an MM energy window of 5 kcal/mol) were optimized at the QM level (B3LYP-D3/6-31+G**). The global minima are shown in Fig. 4. However, if only the local minima of the potential energy surface were taken into account in the calculation of averaged distances using the Boltzmann populations, the experimentally estimated distances could not be reproduced well enough due to the poorly sampled conformational space. Thus, a relaxed rotational scan around the C-5' – N1 bond was performed using a step size of 10° (except for compound **8**, where a step size of 5° was applied) to better sample the conformational space. Since the rotation of the hydroxyl group could significantly perturb the relative energies of the geometry, two torsional scan calculations were finally carried out in each case. These were started from geometries with "opposite" hydroxyl group positions (the hydroxyl groups can be positioned as shown in Fig. 4 and rotated by about 180°). The interproton distances were calculated by averaging the appropriate values of all optimized geometries (2 × 36 structures in each case, 2 × 72 for compound **8a** and **8b**, according to their Boltzmann populations derived from the relative potential energies. These ensemble-averaged distances are listed in Table 4.

By fixing the configuration of C-5′, the configuration of the C-5 center affected mainly the H-5 – H-4′ distance. This was found to be significantly higher when the configurations of these two centers were identical (*R*) in the case of all three compounds.

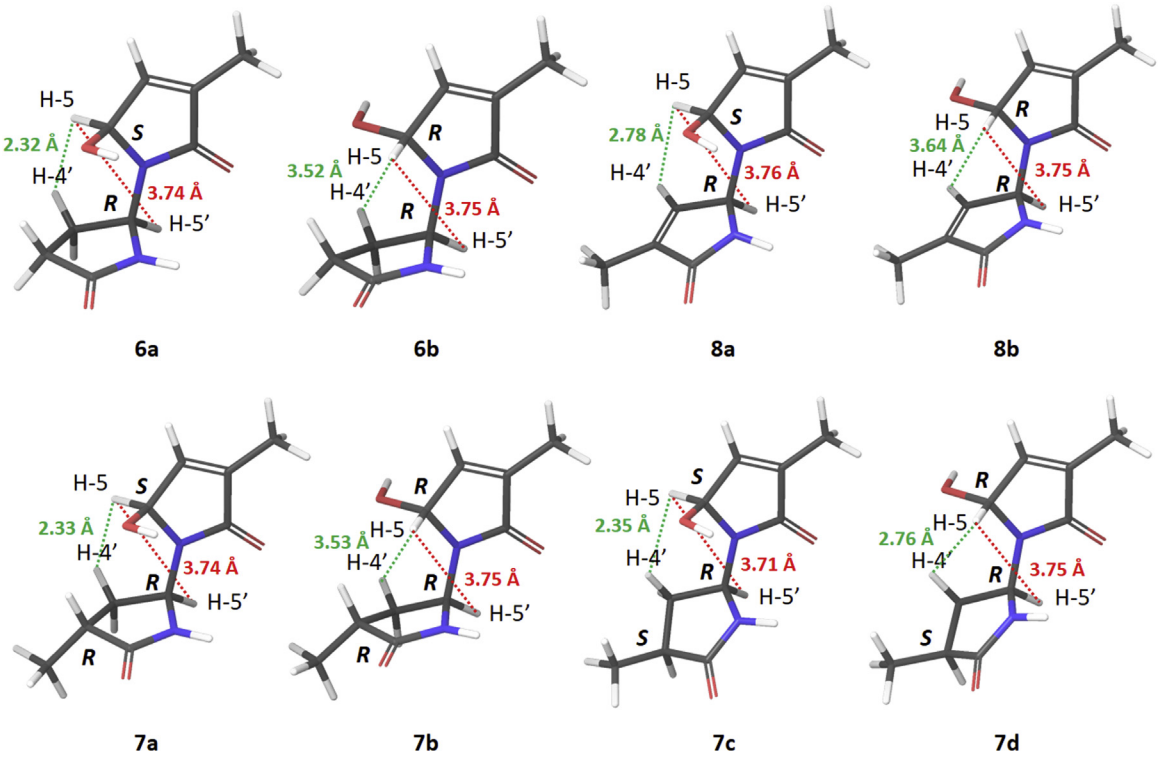

Fig. 4. Lowest energy conformers of the selected enantiomers optimized at the B3LYP-D3/6-31+G** level.

Table 4
Experimentally estimated and calculated proton-proton distances for the selected enantiomers.

Compound	Isomer	Configuration (3′) − 5′ − 5	Distance	Exp. Dist [Å]	Calc. Dist.[Å]	Deviation (Calc. − Exp.) [Å]	Relative error (Deviation/Calc.)
6a	major	R − S	H-5 − H-4′	2.77	2.40	−0.37	−15%
			H-5 − H-5′	3.18	3.34	0.16	+5%
6b	minor	R − R	H-5 − H-4′	3.75	3.55	−0.20	−6%
			H-5 − H-5′	3.24	3.54	0.30	+8%
7a	major trans	R − R − S	H-5 − H-4′	2.73	2.41	−0.32	−13%
			H-5 − H-5′	2.99	3.32	0.33	+10%
7b	minor trans	R − R − R	H-5 − H-4′	3.88	3.54	−0.34	−10%
			H-5 − H-5′	3.33	3.50	0.17	+5%
7c	major cis	S − R − S	H-5 − H-4′	2.57	2.29	−0.28	−12%
			H-5 − H-5′	2.97	3.41	0.44	+13%
7d	minor cis	S − R − R	H-5 − H-4′	3.53	2.92	−0.61	−21%
			H-5 − H-5′	3.30	3.52	0.22	+6%
8a[a]	major	R − S	H-5 − H-4′	2.91	2.82	−0.09	−3%
			H-5 − H-5′	3.31	3.53	0.22	+6%
8b[a]	minor	R − R	H-5 − H-4′	3.87	3.68	−0.19	−5%
			H-5 − H-5′	3.61	3.68	0.07	+2%

[a] Step size in the rotational scan was 5°.

Qualitatively, this can be explained by comparing the appropriate geometries of the lowest energy conformers of the epimeric pairs, as presented in Fig. 4. If the relative position of the pyrroline and pyrrolidine rings of the steroisomers is the same, H-5 occupies "opposite" sides in the stereoisomers, which renders H-5 significantly closer to H-4′ in the 5 S,5′R isomers. On this basis the relative configurations of the stereoisomers (Table 4) could already be assigned with high confidence.

A comparison of the ensemble-averaged (and experimentally estimated) distances showed that the H-5 − H-5′ distances are systematically overestimated (ca. 0.2 Å, 5–13%), while the H-5 − H-4' distances are systematically underestimated (ca. 0.3 Å, 6–21%) by the calculations.

From the modeling perspective these systematic deviations are most probably due to two factors. First, the conformational space sampling of the molecules is still not accurate enough. (This is supported by the significantly lower (2–6%) deviations obtained in the case of **8a** and **8b,** where twice as many conformers (a step-size of 5° instead of 10° in the torsional scan) were taken into account for the distance calculation.) Secondly, due to the H-bond forming capability, a protic and polar solvent such as methanol may significantly affect the conformational space of the studied molecules as well. This however, cannot be taken into account by the continuum solvent models (in our case the Poisson Boltzmann Finite element method (PBF) based calculations). The importance of solvent models when dealing with the accurate *DFT calculations of chemical shifts* has been highlighted recently in the literature [39,40].

From an experimental perspective, the application of different NMR solvents (used in order to obtain NMR data directly comparable to the ones reported in the literature), the omission of the so-called three-spin effect (the presence of a third, nearby proton can corrupt the $\eta \propto d_{I,S}^{-6}$ rule), as well as the integration errors caused by low-level components of the mixtures, may all contribute to the observed deviations between the theoretical and experimental distance values.

Nevertheless, the relative configurations of the C-5/C-5′ centers in the different stereoisomers of the compounds could be confidently determined on the basis of interproton distance measurements and conformational analysis. Since the deviation between the calculated and experimentally determined distances was of systematic nature, the difference obtained for the H-5 − H-4′ distance in the case of the epimeric species could be unambiguously interpreted (compounds **6** and **8**). In the case of **7** (possessing three stereogenic centers), the problem was divided into two subproblems: the relative configuration of C-3′ and C-5′ (cis and trans) were known from 2D NOESY data prior to conformational analysis; subsequently, the decision between **7a** and **7b**, as well as between **7c** and **7d**, *i.e.* the relative configuration of C-5 and C-5′, could be assessed with the aid of the calculations.

To the best of our knowledge, our method of choice for the determination of the relative configuration of small molecules is new, or at least uncommon in the sense that we took into account the full conformational space of the investigated molecule, rather than trying to describe the conformational space with several selected low-energy conformers.

In this way we were able to calculate the ensemble-averaged NOEs (and interproton distances) with a higher accuracy, and we could reliably decide among the diastereomers of the studied molecules.

2.2. Assigning the relative configuration of lily alkaloids

The application of identical solvents (or solvent mixtures) enabled the direct comparison of our NMR data (^{1}H chemical shifts and coupling constants) of the synthetic products with those reported for lily alkaloids isolated from natural sources [11–14,17]. With regard to **4** and **5** the measured ^{1}H NMR chemical shifts agreed well with the literature data [11]. A comparison of the ^{1}H−^{1}H coupling constants (cf. Ref. [17]) reported for lilaline and determined for the two diasteromers of **14** (Table 5) showed that the natural product possesses the same relative configuration as our major synthetic product, (3″*R**,5″*S**)-**14** (Fig. 5) with the functional groups of the pyrrolinone ring having a trans arrangement; the coupling constants in our dataset and the dataset in the literature differed from each other by less than 0.2 Hz. The (3″*R**,5″*R**)-**14** diastereomer, which shows a completely different coupling pattern in the ^{1}H NMR spectrum, is a new synthetic compound.

A similar comparison to the reported NMR data [12,13] in the case of **6** (Table 6) and **8** (Table 7) led to the conclusion that the compounds isolated from natural sources have the same relative configurations as our major synthetic stereoisomers, (5*S**,5′*R**)-5-hydroxy-3-methyl-1-(2′-oxopyrrolidin-5′-yl)-3-pyrrolin-2-one (**6a**), and (5*S**,5′*R**)-5-hydroxy-3-methyl-1-(3′-methyl-2′-oxo-3′-pyrrolin-5′-yl)-3-pyrrolin-2-one (**8a**). The measured ^{1}H NMR chemical shifts and coupling constants and the values reported in the literature differed from each other by less than 0.01 ppm and 0.2 Hz, respectively. The other synthetic diastereomers (**6b** and **8b**) are new compounds.

In the case of compound **7** however, ambiguities were found between the reported [11] and observed spectral data (Table 8). In particular the chemical shifts of H-4, C(5)-O<u>H</u> and H-1′ reported by Haladová et al. were ca. 0.4 ppm downfield of those observed for any of the synthetic isomers. It should be noted however that the reported chemical shifts are inconsistent with the data reported for close structural analogues in the same publication as well. Due to this discrepancy, in the case of compound **7** the relative configuration of the real lily alkaloid can only be given speculatively. By accepting the plausible reasoning that the inconsistency in the NMR data arises simply from the use of a different NMR solvent, a tentative assignment can be given. Based on the reported similar coupling constants, an identical relative configuration of C-3′ and C-5′ can be suggested in the natural product as it was determined in lilaline **14**. Assuming that the formation of **7** is governed by a similar metabolic pathway that leads to **6** in the plants, the relative configuration of C-5 and C-5′ is likely to be the same. On this basis the naturally occurring alkaloid can most probably be described by the same relative stereochemistry as our main synthetic stereoisomer **7a** (Fig. 5): *rel*-(5*S*,3′*R*,5′*R*)-5-hydroxy-3-methyl-1-(3′-methyl-2′-oxopyrrolidin-5′-yl)-3-pyrrolin-2-one. The other diastereomers of **7** are new synthetic derivates; they have not been reported in the literature.

3. Conclusion

In the present work we accomplished the synthesis of five racemic pyrroline alkaloids as well as the flavonoid alkaloid lilaline, which were all isolated earlier from *Lilium candidum* L. These compounds were synthesized from cheap, easily accessible starting materials via *Mannich*-type alkylations employing cyclic *N*-acylaminocarbinols as electrophile precursors. The synthesized lily alkaloids were isolated as racemates or mixtures of diastereomers in different compositions. The relative configuration of some lily alkaloids was determined by the concerted use of NMR-based interproton distance measurements and conformational analyses at the DFT level. To the best of our knowledge, our method of choice for the determination of the relative configuration of flexible

Table 5
Comparison of the literature ^{1}H NMR data for **14** with our data for **14a** and **14b**.

^{1}H NMR data	*Lilium candidum* L.	Synthetic products	
	literature data [17]	(3″*R**,5″*S**)-**14** = *trans*-**14** (major, 76%)	(3″*R**,5″*R**)-**14** = *cis*-**14** (minor, 24%)
Position	δ_H (ppm) (apparent multiplicity; estimated *J* coupling constants in Hz)		
H-6	6.24 (s)	6.26 (s)	6.25 (s)
H-2′, H-6′	8.01 (d; 9.0)	7.95 (m)	7.98 (m)
H-3′, H-5′	6.91 (d; 9.0)	6.89 (m)	6.85 (m)
NH-1″	–	7.67 (br)	7.83 (br)
H-3″	2.77 (dqd; 9.7, 7.4, 4.9)	2.54 (dqd; 9.6, 7.4, 5.0)	2.48 (ddq; 11.5, 8.4, 7.0)
C(3″)-CH_3	1.29 (d; 7.4)	1.13 (d; 7.4 Hz)	1.05 (d; 7.0)
H_2-4″	2.17 (ddd; 12.9, 8.9, 4.9)	1.99 (ddd; 12.7, 8.8, 5.0)	1.94 (ddd; 11.9, 11.5, 10.0)
	2.57 (ddd; 12.9, 9.7, 5.9)	2.38 (ddd; 12.7, 9.6, 5.9)	2.34 (ddd; 11.9, 8.4, 6.6)
H-5″	5.56 (dd; 8.9, 5.9)	5.35 (dd; 8.8, 5.9)	5.26 (dd; 10.0, 6.6)

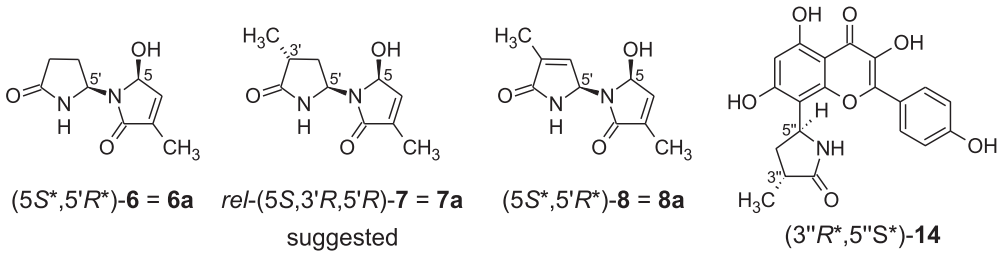

Fig. 5. Relative configurations of lily alkaloids determined by NMR and molecular modeling.

Table 6
Comparison of the literature ^{1}H NMR data for **6** with our data for **6a** and **6b**.

^{1}H NMR data in acetone-d_6: methanol-d_4 = 1:1	*Lilium candidum* L.	Synthetic products	
	literature data [12]	(5*S**,5′*R**)-**6** = **6a** (major, 79%)	(5*R**,5′*R**)-**6** = **6b** (minor, 21%)
Position	δ_H (ppm) (apparent multiplicity; estimated *J* coupling constants in Hz)		
C(3)-C<u>H</u>$_3$	1.83 (dd; 1.8, 1.4)	1.82 (t; 1.6)	1.83 (t; 1.6)
H-4	6.68 (dq; 1.8, 1.8)	6.67 (qui; 1.7)	6.68 (qui; 1.7)
H-5	5.53 (dq; 1.8, 1.4)	5.54 (m)	5.48 (m)
H_2-3′	2.29 (m)	2.30 (m)	2.27 (m)
	2.75 (m)	2.75 (m)	2.69 (m)
H_2-4′	2.34 (m)	2.35 (m)	2.38 (m)
	2.57 (m)	2.57 (m)	2.51 (m)
H-5′	5.51 (dd; 8.7, 2.4)	5.51 (dd; 8.7, 2.4)	5.73 (dd; 8.5, 2.5)

qui: quintet.

Table 7
Comparison of the literature ^{1}H NMR data for **8** with our data for **8a** and **8b**.

^{1}H NMR data in methanol-d_4	*Lilium candidum* L.	Synthetic products	
	literature data [13]	(5*S**,5′*R**)-**8** = **8a** (major, 75%)	(5*R**,5′*R**)-**8** = **8b** (minor, 25%)
Position	δ_H (ppm) (apparent multiplicity; estimated *J* coupling constants in Hz)		
C(3)-C<u>H</u>$_3$	1.85 (dd; 1.7, 1.4)	1.85 (dd; 1.7, 1.5)	1.86 (dd; 1.7, 1.4)
H-4	6.64 (dqd; 1.8, 1.7, 0.4)	6.64 (quid; 1.7, 0.3)	6.67 (quid; 1.8, 0.5)
H-5	5.40 (dqd; 1.8, 1.4, 0.3)	5.40 (qui; 1.5)	5.25 (qui; 1.3)
C(3′)-C<u>H</u>$_3$	1.91 (dd; 1.7, 1.7)	1.90 (t; 1.7)	1.88 (t; 1.8)
H-4′	6.76 (dq; 2.0, 1.7)	6.76 (qui; 1.8)	6.78 (qui; 1.8)
H-5′	5.96 (dqdd; 2.0, 1.7, 0.4, 0.3)	5.96 (qui; 1.8)	6.11 (qui; 1.8)

qui: quintet.

Table 8
Comparison of the literature ^{1}H NMR data for **7** with our data for **7a**–**7d**.

^{1}H NMR data in acetone-d_6	*Lilium candidum* L.	Synthetic products			
	literature data [11]	*rel*-(5*S*,3′R,5′R)-**7** = **7a** (53%)	*rel*-(5*R*,3′R,5′*R*)-**7** = **7b** (35%)	*rel*-(5*S*,3′S,5′*R*)-**7** = **7c** (7%)	*rel*-(5*R*,3′S,5′*R*)-**7** = **7d** (5%)
Position	δ_H (ppm) (apparent multiplicity; estimated *J* coupling constants in Hz)				
C(3)-C<u>H</u>$_3$	1.77 (dd; 1.8, 1.3)	1.77 (t; 1.5)	1.77 (t; 1.5)	≈1.78 (om)	≈1.78 (om)
H-4	6.20 (qd; 1.8, 1.8)	6.63 (qui; 1.7)	≈6.64 (qui; 1.8)	≈6.64 (om)	≈6.64 (om)
H-5	5.54 (ddq; 10.1, 1.8, 1.3)	5.58 (dqui; 10.0, 1.5)	5.50 (dqui; 10.0, 1.4)	5.63 (om)	5.64 (om)
C(5)-O<u>H</u>	4.83 (d; 10.1)	5.24 (d; 10.0)	5.22 (d; 10.0)	5.36 (d; 9.4)	5.33 (d; 9.6)
NH-1′	6.86 (br s; 1.4, 0.8)	~7.30 (br)	~7.38 (br)	–	–
H-3′	2.85 (ddq; 9.5, 8.7, 7.2)	2.92 (ddq; 9.1, 8.9, 7.3)	2.88 (ddq; 9.2, 8.9, 7.2)	2.51 (om)	2.49 (om)
C(3′)-C<u>H</u>$_3$	1.12 (d; 7.2)	1.133 (d; 7.3)	1.127 (d; 7.2)	1.22 (d; 7.1)	1.20 (d; 6.9)
H_2-4′	2.10 (ddd; 13.7, 9.5, 8.5)	2.11 (ddd; 13.6, 8.9, 8.6)	2.07 (ddd; 13.3, 9.2, 8.6)	2.17 (ddd; 12.7, 9.1, 7.2)	2.39 (ddd; 12.4, 9.6, 7.4)
	2.54 (dddd; 13.7, 8.7, 1.4, 0.8)	2.54 (ddd; 13.6, 9.1, 1.2)	2.55 (dddd; 13.3, 8.9, 1.2, 0.4)	2.58 (ddd; 12.7, 9.3, 7.6)	2.51 (om)
H-5′	5.40 (ddd; 8.5, 1.4, 1.4)	5.45 (ddd; 8.6, 1.4, 1.2)	5.62 (ddd; 8.6, 1.4, 1.2)	5.57 (dd; 7.6, 7.2)	5.68 (t; 7.4)

qui: quintet.
om: overlapping multiplet.

compounds is uncommon in the sense that it is based on mapping the full conformational space in order to obtain reliable results, rather than arbitrarily restricting the conformational space to several representative conformers.

4. Experimental section

Melting points were measured on a SANYO Gallenkamp apparatus and are uncorrected. IR spectra were recorded on a Bruker FT-IR instrument and a PerkinElmer Spectrum 100 FT-IR Spectrometer equipped with Universal ATR (diamond/ZnSe) accessory. NMR measurements (^{1}H, ^{13}C, COSY, 1D NOESY, 1D ROESY, 2D ROESY, HSQC, HMBC, 1,1-ADEQUATE) were performed on Varian VNMRS 400 MHz (equipped with 5 mm OneNMR ^{15}N–^{31} P/{^{1}H–^{19}F} PFG Probe), Varian VNMRS 500 MHz (equipped with ^{1}H{^{13}C,^{15}N} 5 mm PFG Triple Resonance ^{13}C Enhanced Cold Probe) and Varian VNMRS 800 MHz (equipped with ^{1}H{^{13}C,^{15}N} Triple Resonance ^{13}C Enhanced Salt Tolerant Cold Probe), Bruker Avance III HDX 500 MHz (equipped with ^{1}H {^{13}C,^{15}N} 5 mm TCI CryoProbe), and Bruker Avance III HDX 800 MHz (equipped with ^{1}H/^{19}F {^{13}C,^{15}N} 5 mm TCI CryoProbe) spectrometers. ^{1}H and ^{13}C chemical shifts are given on the delta scale in parts per million (ppm) relative to tetramethylsilane (TMS). ^{1}H multiplicities are given as d (doublet), t (triplet), q (quartet), spt (septet) and their combinations or as m (multiplet); br corresponds to broad. Coupling constants are given in Hz in descending order. NMR spectra were processed using VnmrJ 2.2 Revision C (Varian, Inc., Palo Alto, CA, USA), Bruker TopSpin 3.5 pl 6 (Bruker Corporation, Billerica, MA, USA) and ACD/Spectrus Processor version 2017.1.3 (Advanced Chemistry Development, Inc., Toronto, ON, Canada); Daisy plugin of TopSpin was used for spin system simulations. HRMS and MS analyses were performed on a Finnigan MAT 95 XP and a Thermo LTQ FT Ultra as well as a Thermo LTQ XL (Thermo Fisher Scientific, Bremen, Germany) system. The ionization method was EI operated in positive ion mode on a Finnigan MAT 95 XP. The electron energy was 70 eV and the source temperature was set to 220 °C. The ionization method was ESI operated in positive ion mode on the other two systems. For the CID experiment helium was used as the collision gas, and normalized collision energy (expressed in percentage), which is a measure of the amplitude of the resonance excitation RF voltage applied to the endcaps of the linear ion trap, was used to induce fragmentation. The protonated molecular ion peaks were fragmented by CID at a normalized collision energy of 35%. Data acquisition and analysis were accomplished with Xcalibur software version 2.0 (Thermo Fisher Scientific). TLC was carried out on TLC Silica gel 60 F_{254} on 20 × 20 cm aluminium sheets (Merck), and preparative TLC was carried out using Silica gel 60 $PF_{254+366}$ (Merck) coated glass plates. Column chromatography was performed using Silica gel 60 (0.063–0.200 mm) (Merck). Kaempferol was purchased from Xi'an Lyphar Biotech Co., Ltd (Xi'an, Shaanxi, China) and used without further purification.

4.1. 1-(Triisopropylsilyl)pyrrole (**21**)

To a solution of pyrrole (5.17 mL, 5.00 g, 74.5 mmol) in dry THF (100 mL) at −75 °C, n-butyllithium solution (33.0 mL, 2.5 M soln. In hexanes, 82.5 mmol) was slowly added under argon. The solution was stirred at −75 °C for 10 min, then triisopropylsilyl chloride (16.0 mL, 14.4 g, 74.8 mmol) was added over 10 min. After the addition, the mixture was let to warm up to room temperature, then it was quenched with water (100 mL). The mixture was extracted with diethyl ether (3 × 50 mL). The ether solution was dried (Na_2SO_4), then the solvent was removed under reduced pressure, giving the title compound **21** as a colorless oil (16.5 g, 99%), R_f (hexane:EtOAc = 1:4) 0.95; ν_{max} (neat film) 2946, 2892, 2867, 1460, 1185, 1081, 1045 cm^{-1}.^{1}H NMR (500 MHz, $CDCl_3$) δ (ppm) 1.10 (18H; d; J = 7.5 Hz; CH_3); 1.45 (3H; spt; J = 7.5 Hz; C<u>H</u>$(CH_3)_2$); 6.30–6.33 (2H; m; H-3, H-4); 6.77–6.82 (2H; m; H-2, H-5). ^{13}C NMR (126 MHz, $CDCl_3$) δ (ppm) 11.7 (C<u>H</u>$(CH_3)_2$); 17.8 (CH_3); 110.0 (C-3, C-4); 124.0 (C-2, C-5). Lit. ^{1}H NMR (500 MHz, $CDCl_3$) δ (ppm) 1.09 (18 H; d; J = 7.4 Hz; CH_3); 1.45 (3H; spt; J = 7.4 Hz; C<u>H</u>$(CH_3)_2$); 6.32 (2H; t*; H-3, H-4); 6.80 (2H; t*; H-2, H-5); *should be interpreted as apparent multiplicity; no coupling constants were reported [23].

21

4.2. Pyrrole-3-carboxaldehyde (**22**)

Phosphoryl chloride (8.27 mL, 13.6 g, 88.7 mmol) was cooled to 0 °C with stirring, then DMF (6.86 mL, 6.50 g, 88.9 mmol) was slowly added at 0 °C. To this mixture a solution of 1-(triisopropylsilyl)pyrrole (**21**) (16.5 g, 73.8 mmol) in acetonitrile (60 mL) was added over 30 min. The reaction mixture was let to warm up to room temperature and was stirred for 2 h, then it was again cooled to 0 °C. The mixture was quenched with 2 M NaOH solution until pH = 9. The mixture was extracted with diethyl ether (3 × 30 mL). The ether solution was dried (Na_2SO_4), then the solvent was removed under reduced pressure. The crude product was purified by column chromatography, using hexane:EtOAc (1:4) as the eluent, giving the title compound **22** as a pale brown crystalline solid (4.56 g, 65%), mp 65 °C (lit.: 68 °C) [23]; R_f (hexane:EtOAc = 1:4) 0.63; ν_{max} (KBr) 3258, 3116, 1653, 1505, 1435, 1416, 1402, 1377, 1297, 1091, 1061, 1052 cm^{-1}; ^{1}H NMR (800 MHz, $CDCl_3$) δ (ppm) 6.69–6.70 (1H; m; H-4); 6.85–6.87 (1H; m; H-5); 7.47–7.48 (1H; m; H-2); 9.20–9.54 (1H; br m; NH); 9.82 (1H; ~s; CHO). ^{13}C NMR (201 MHz, $CDCl_3$) δ (ppm) 107.5 (C-4); 120.7 (C-5); 126.7 (C-3); 127.4 (C-2); 186.1 (CHO). EI-HRMS: M = 95.0353 (C_5H_5ON; calc.: 95.0366); EI-MS (rel. int. %): 95(100); 66(16).

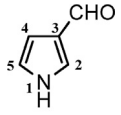

22

4.3. 3-Methylpyrrole (**23**)

To a solution of KOH (10.8 g, 192 mmol) in ethylene glycol (72 mL) a solution of pyrrole-3-carboxaldehyde (**22**) (4.56 g, 47.9 mmol) was added in hydrazine hydrate (2.33 mL, 2.40 g, 48.0 mmol). The flask was fitted for distillation, and the mixture was slowly heated to 200 °C with vigorous stirring. The pure fractions of the product were collected at 140–145 °C. The distillate was extracted with diethyl ether (3 × 30 mL). The ether solution was dried (Na_2SO_4), then the solvent was removed under reduced pressure, giving the title compound **23** as a colorless liquid (2.84 g, 73%), bp 143–145 °C (lit.: 142–143 °C) [41]; R_f (hexane:EtOAc = 4:1) 0.60; ν_{max} (neat film) 3387, 3091, 2924, 2867, 2744, 1601, 1560, 1485, 1429, 1254, 1137, 1059 cm^{-1}; ^{1}H NMR (800 MHz; $CDCl_3$) δ (ppm) 2.19 (3H; s; CH_3); 6.12–6.13 (1H; m; H-4); 6.59–6.61 (1H; m; H-2); 6.74–6.76 (1H; m; H-5); 7.82–8.18 (1H; br m; NH). ^{13}C NMR (201 MHz; $CDCl_3$) δ (ppm) 11.7 (CH_3); 109.6 (C-4); 115.5 (C-2); 117.7 (C-5); 118.7 (C-3). EI-HRMS: M = 81.0571 (C_5H_7N; calc.: 81.0573); EI-MS (rel. int. %): 81(65); 80(100); 53(21).

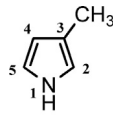

23

4.4. 3-Methyl-3-pyrrolin-2-one (**17**)

30% Hydrogen peroxide (6.90 mL, 67.6 mmol) was added to 3-methylpyrrole (**23**) (2.84 g, 35.0 mmol) at room temperature, and the mixture was vigorously stirred for 24 h. The mixture was extracted with diethyl ether (6 × 20 mL), the ether solution was dried (Na_2SO_4), then the solvent was evaporated under reduced pressure. The crude product was recrystallized from acetone, giving the title compound **17** as a pale yellow crystalline solid (1.80 g, 53%), mp 87–89 °C (lit.: 95–96 °C) [26]; R_f (acetone) 0.55; ν_{max} (KBr) 3215, 3068, 2971, 2923, 2855, 1683, 1640, 1447, 1363, 1231, 1170, 1077 cm^{-1}; ^1H NMR (400 MHz; DMSO-d_6) δ (ppm) 1.71–1.75 (3H; m; C(3)-C$\underline{H}_3$); 3.75–3.79 (2H; m; H_2-5); 6.84–6.88 (1H; m; H-4); 8.01–8.23 (1H; br; NH-1). ^{13}C NMR (101 MHz; DMSO-d_6) δ (ppm) 10.7 (C(3)-$\underline{C}H_3$); 45.6 (C-5); 134.0 (C-3); 138.6 (C-4); 173.8 (C-2). EI-HRMS: M = 97.0519 (C_5H_7ON; calc.: 97.0528); EI-MS (rel. int. %): 97(100); 82(11); 78(5); 69(15); 68(17); 54(4).

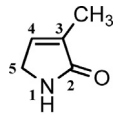

17

4.5. 5-Ethoxypyrrolidin-2-one (**18**)

To a solution of succinimide (24) (7.16 g, 72.3 mmol) in ethanol (300 mL) at 0 °C was added sodium borohydride (4.00 g, 106 mmol) in one portion. The reaction mixture was stirred at 0 °C for 4 h, during which time every 15 min five drops of 2 M ethanolic hydrogen chloride solution were added. Then the reaction mixture was acidified to pH = 3 with 2 M ethanolic hydrogen chloride solution over 30 min, after which it was stirred at 10 °C for 90 min. Then the reaction mixture was neutralised (pH = 7) with 5% ethanolic potassium hydroxide solution and evaporated in vacuo to give a syrupy solid, which was suspended in chloroform (80 mL), filtered, and the precipitate washed with chloroform (3 × 20 mL). The filtrate was evaporated in vacuo to give a colourless oil, which was dissolved in dichloromethane (80 mL) and washed with water (3 × 10 mL). The aqueous phase was extracted with dichloromethane (6 × 20 mL), then the organic phases were unified, dried ($MgSO_4$) and the solvent evaporated in vacuo to give the title compound 18 (5.79 g, 62%) as a colourless oil, which crystallized on standing, giving white crystals, mp 54–58 °C (lit.: 48–53 °C) [22]; Rf (acetone) 0.72; ν_{max} (KBr) 3200, 2978, 1707, 1689, 1668, 1457, 1282, 1250, 1067, 986 cm^{-1}; ^1H NMR (400 MHz; DMSO-d_6) δ (ppm) 1.78–1.89 (1H; m; H^x-4); 1.95–2.05 (1H; m; H^x-3); 2.11–2.30 (2H; m; H^y-3, H^y-4); 3.27–3.35 (1H; m), 3.44–3.54 (1H; m) (OCH_2); 4.83–4.89 (1H; m; H-5); 8.62 (1H; s; NH-1); ^{13}C NMR (101 MHz; DMSO-d_6) δ (ppm) 15.1 (CH_3); 27.7 (C-4); 28.1 (C-3); 61.6 (OCH_2); 85.0 (C-5); 177.4 (C-2); ESI-MS: M+H = 130 ($C_6H_{12}O_2N$); ESI-MS-MS (CID = 35%, rel. int. %): 84(100).

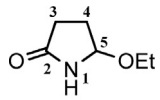

18

4.6. Citraconimide (**26**)

To a solution of citraconic anhydride (**25**) (12.0 g, 107 mmol) in DMF (100 mL) at 100 °C hexamethyldisilazane (34.2 mL, 160 mmol) was added. The mixture was stirred at 100 °C for 1 h, then it was cooled to room temperature. The solvent was evaporated under reduced pressure. The crude product was recrystallized from a mixture of hexane and ethyl acetate to give the title compound **26** as a white crystalline solid (8.33 g, 70%), mp 104–105 °C (lit.: 104–105 °C) [3]; R_f (DCM:MeOH = 10:1) 0.71; ν_{max} (KBr) 3271, 3098, 2674, 1844, 1778, 1764, 1712, 1634, 1342, 1284, 1175, 1090 cm^{-1}; ^1H NMR (500 MHz; DMSO-d_6) δ (ppm) 1.94 (3H; d; J = 1.8 Hz; C(3)-C$\underline{H}_3$); 6.50 (1H; q; J = 1.8 Hz; H-4); 10.72 (1H; br s; NH-1); ^{13}C NMR (126 MHz; DMSO-d_6) δ (ppm) 10.2 (C(3)-$\underline{C}H_3$); 128.0 (C-4); 145.9 (C-3); 172.2 (C-5); 173.1 (C-2); HRMS: M = 111.0311 ($C_5H_5O_2N$; delta = −8.1 ppm); HR-EI-MS (rel. int. %): 111(100); 83(8); 68(39).

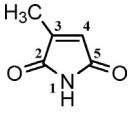

26

4.7. (±)-Jatropham [5-hydroxy-3-methyl-3-pyrrolin-2-one] (**1**)

To a solution of citraconimide (**26**) (1.00 g, 9.00 mmol) in THF (50 mL) under nitrogen at −78 °C diisobutyl aluminium hydride solution (10.7 mL, 16.0 mmol, 25 wt % in toluene) was added via a syringe. The mixture was let to warm up to 0 °C and it was stirred at this temperature for a further 90 min, then it was quenched with a mixture of methanol (25 mL) and water (25 mL). The solvents were evaporated under reduced pressure, then the crude product was triturated in ethyl acetate. The suspension was filtered, the filtrate was dried (Na_2SO_4) and evaporated under reduced pressure to give the title compound **1** as a white crystalline solid (930 mg, 91%), mp 115–117 °C (lit.: 115–118 °C) [5]; R_f (DCM:MeOH = 10:1) 0.42; ν_{max} (KBr) 3244, 2985, 2931, 1688, 1650, 1409, 1306, 1281, 1216, 1058 cm^{-1}; ^1H NMR (500 MHz; CD_3OD) δ (ppm) 1.83 (3H; dd; J = 1.7; 1.4 Hz; C(3)-C$\underline{H}_3$); 5.44 (1H; dq; 1.7; 1.4 Hz; H-5); 6.63 (1H; ~qui; J = 1.7 Hz; H-4); ^{13}C NMR (126 MHz; CD_3OD) δ (ppm) 10.6 (C(3)-$\underline{C}H_3$); 80.0 (C-5); 136.9 (C-3); 143.1 (C-4); 175.5 (C-2); HRMS: M+H = 114.05495 (delta = −0.04 ppm; $C_5H_8O_2N$); HR-ESI-MS-MS (CID = 55%, rel. int. %): 97(100).

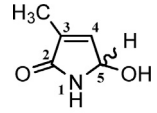

1

4.8. (±)-2-Methylsuccinimide (**27**)

To a solution of citraconimide (**26**) (4.50 g, 40.5 mmol) in ethanol (50 mL) 10% palladised charcoal (2.00 g) was added. The suspension was hydrogenated under atmospheric pressure for 4 h.

After completion of the reaction (confirmed with TLC) the mixture was filtered through a pad of Celite, the Celite layer was washed with ethanol (2 × 20 mL), and the filtrate was evaporated under reduced pressure, giving the title compound **27** as a white crystalline solid (4.55 g, 99%), mp 57–59 °C (lit.: 65 °C) [42]; R_f (DCM:MeOH = 10:1) 0.52; ν_{max} (KBr) 3201, 3071, 2766, 1763, 1707, 1352, 1206, 1176, 1037 cm^{-1}; ^1H NMR (400 MHz; DMSO-d_6) δ (ppm) 1.16 (3H; d; J = 7.2 Hz; C(3)-C$\underline{H}_3$); 2.26 (1H; m; ^2J = −17.7 Hz (H^a-4), ^3J = 5.1 Hz (H-3); H^b-4); 2.78 (1H; m; ^3J = 9.2 Hz (H-3); H^a-4); 2.81 (1H; m; ^3J = 7.3 Hz (C(3)-CH_3); H^a-4); 10.94–11.10 (1H; br; NH-1); ^{13}C NMR (101 MHz; DMSO-d_6) δ (ppm) 15.7 (C(3)-$\underline{C}H_3$); 35.4 (C-3); 37.1 (C-4); 178.0 (C-5); 182.2 (C-2); HRMS: M = 113.0461 (delta = −14.2 ppm; $C_5H_7NO_2$); HR-EI-MS (rel. int. %): 113(100); 70(77).

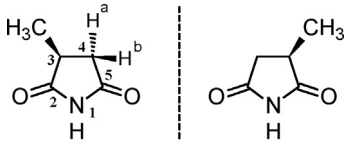

(±)-**27**

4.9. 5-Hydroxy-3-methylpyrrolidin-2-one (**19**)

To a solution of (±)-2-methylsuccinimide (**27**) (1.00 g, 8.84 mmol) in THF (50 mL) at −78 °C diisobutyl aluminium hydride solution (10.7 mL, 16.0 mmol, 25% in toluene) was added via a syringe. The mixture was let to warm up to 0 °C and was stirred at this temperature for a further 90 min. Then it was quenched with a mixture of methanol (25 mL) and water (25 mL). The solvents were evaporated under reduced pressure, then the crude product was triturated in ethyl acetate. The suspension was filtered, the filtrate was dried (Na_2SO_4) and evaporated under reduced pressure to give the title compound **19** (contaminated with 27% of the minor isomer **28**) as a colorless oil (737 mg, 72%), R_f (DCM:MeOH = 10:1) 0.54; ν_{max} (neat film) 3268, 2967, 2935, 1664, 1458, 1335, 1254, 1107, 1054, 1000 cm^{-1}. HRMS: 2M+Na = 253.11569 (delta = −0.74 ppm; $C_{10}H_{18}O_4N_2Na$); HR-ESI-MS-MS (CID = 35%, rel. int. %): 235(47); 233(11); 138(100).

((3*S**,5*S**)-**19**): ^1H NMR (800 MHz; DMSO-d_6) δ (ppm) 1.00 (3H; d; J = 7.2 Hz; C(3)-C$\underline{H}_3$); 1.76 (1H; ddd; J = 13.2; 9.5; 6.1 Hz; H^b-4); 1.99 (1H; dd; J = 13.2; 8.2 Hz; H^a-4); 2.44–2.49 (1H; m; H-3); 4.97 (1H; br d; J = 6.1 Hz; H-5); 5.64 (1H; br; C(5)-O$\underline{H}$); 8.18 (1H; br; NH-1); ^{13}C NMR (201 MHz; DMSO-d_6) δ (ppm) 15.7 (C(3)-$\underline{C}H_3$); 32.9 (C-3); 39.2 (C-4); 76.1 (C-5); 179.1 (C-2).

((3*S**,5*R**)-**19**): ^1H NMR (500 MHz; DMSO-d_6) δ (ppm) 1.09 (3H; d; J = 7.3 Hz; C(3)-C$\underline{H}_3$); 1.35 (1H; ddd; J = 13.2; 6.8; 4.0 Hz; H^b-4); 2.20 (1H; dqd; J = 9.2; 7.3; 6.8 Hz; H-3); 2.43–2.47 (1H; m; H^a-4); 5.05 (1H; dd; J = 6.3; 4.0 Hz; H-5); 5.74 (1H; d; J = 6.9 Hz; C(5)-O$\underline{H}$); 8.08 (1H; br; NH-1); ^{13}C NMR (201 MHz; DMSO-d_6) δ (ppm) 17.0 (C(3)-$\underline{C}H_3$); 35.0 (C-3); 38.6 (C-4); 77.1 (C-5); 178.1 (C-2).

((4*S**,5*R**)-**28**): ^1H NMR (800 MHz; DMSO-d_6) δ (ppm) 0.98 (3H; d; J = 7.1 Hz; C(4)-C$\underline{H}_3$); 1.64 (1H; dd; J = 16.6, 4.1 Hz; H^b-3); 2.01–2.06 (1H; m; H-4); 2.47 (1H; dd; J = 16.6, 8.3 Hz; H^a-3); 4.60 (1H; ddd; J = 6.9, ~2.1, ~1.1 Hz; H-5); 5.74 (1H; d; J = 6.9 Hz; C(5)-O$\underline{H}$); 8.11 (1H; br; NH-1); ^{13}C NMR (201 MHz; DMSO-d_6) δ (ppm) 18.4 (C(4)-$\underline{C}H_3$); 36.8 (C-3); 37.7 (C-4); 85.0 (C-5); 175.7 (C-2).

((4*S**,5*S**)-**28**): ^1H NMR (800 MHz; DMSO-d_6) δ (ppm) 0.95 (3H; d; J = 6.9 Hz; C(4)-C$\underline{H}_3$); 1.90 (1H; dd; J = 16.2, 10.6 Hz; H^b-3); 2.04 (1H; dd; J = 16.2, 8.4 Hz; H^a-3); 2.31 (1H; ddqd; J = 10.6, 8.4, 6.9, 5.4 Hz; H-4); 4.84 (1H; ddd; J = 7.4, 5.4, 1.2 Hz; H-5); 5.43 (1H; d; J = 7.4 Hz; C(5)-O$\underline{H}$); 8.17 (1H; br; NH-1); ^{13}C NMR (201 MHz; DMSO-d_6) δ (ppm) 13.9 (C(4)-$\underline{C}H_3$); 34.3 (C-4); 35.0 (C-3); 79.9 (C-5); 176.8 (C-2).

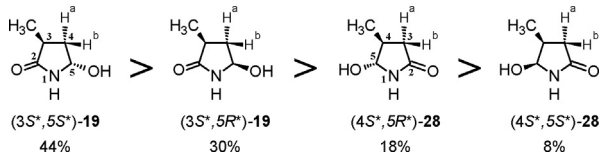

4.10. 3-Methyl-1-(2′-oxopyrrolidin-5′-yl)-3-pyrrolin-2-one (**4**)

To a solution of 3-methyl-3-pyrrolin-2-one (**17**) (106 mg, 1.09 mmol) in THF (2 mL) 5-ethoxypyrrolidin-2-one (**18**) (141 mg, 1.09 mmol) and *p*-toluenesulfonic acid monohydrate (13.0 mg, 68.3 μmol) were added. The mixture was stirred at room temperature for 1 h, after which a white crystalline solid precipitated. The mixture was cooled to 0 °C and the product was filtered. The crystals were washed with cold acetone and dried by suction, giving the title compound **4** as a white crystalline solid (107 mg, 54%), mp 164–166 °C (lit.: 167–169 °C) [11]; R_f (acetone) 0.38; ν_{max} (KBr) 3189, 3096, 2916, 1707, 1672, 1462, 1378, 1271, 1240, 1190, 1174, 1094 cm^{-1}; ^1H NMR (500 MHz; acetone-d_6) δ (ppm) 1.79 (3H; m; ^5J = 2.1 Hz (H^a-5), ^5J = 2.0 Hz (H^b-5), ^4J = 1.7 Hz (H-4); C(3)-C$\underline{H}_3$); 2.08 (1H; m; ^2J = −13.7 Hz (H^a-4′), ^3J = 9.8 Hz (H^b-3′), ^3J = 4.6 Hz (H^a-3′), ^3J = 3.3 Hz (H-5′); H^b-4′); 2.22 (1H; m; ^2J = −17.1 Hz (H^b-3′), ^3J = 10.2 Hz (H^a-4′); H^a-3′); 2.44 (1H; m; ^3J = 7.7 Hz (H^a-4′); H^b-3′); 2.50 (1H; m; ^3J = 7.6 Hz (H-5′); H^a-4′); 3.91 (1H; m; ^2J = −19.4 Hz (H^b-5); ^3J = 1.4 Hz (H-4); H^a-5); 3.98 (1H; m; ^3J = 2.4 Hz (H-4); H^b-5); 5.80 (1H; m; H-5′); 6.88 (1H; m; H-4); 7.20 (1H; br; NH-1′); ^{13}C NMR (126 MHz; acetone-d_6) δ (ppm) 11.1 (C(3)-$\underline{C}H_3$); 26.7 (C-4′); 29.6 (C-3′); 46.4 (C-5); 62.5 (C-5′); 135.2 (C-3); 137.6 (C-4); 172.0 (C-2); 177.0 (C-2′); Lit. ^1H NMR [11]: 1.78 (3H; ddd; ^5J = 2.0 Hz (H^x-5), ^5J = 2.0 Hz (H^y-5), ^4J = 1.8 Hz (H-4); C(3)-CH_3); 2.02–2.56 (4H; m; H_2-3′, H_2-4′); 3.90 (1H; m; ^2J = 19.3 Hz (H^y-5), ^3J = 2.0 Hz (H-4); H^x-5); 3.96 (1H; m; ^3J = 2.0 Hz (H-4); H^y-5); 5.79 (1H; m; ^3J = 7.8 Hz (H^x-4′), ^3J = 3.3 Hz (H^y-4′), ^3J = 1.3 Hz (NH-1′), ^5J = 0.6 Hz (H-4), ^4J = 0.5 Hz (H^x-5), ^4J = 0.5 Hz (H^y-5); H-5′); 6.86 (1H; ddqd; H-4); 7.07 (br s, 1H, NH-1′); ESI-MS: M+H = 181 ($C_9H_{13}O_2N_2$); ESI-MS-MS (CID = 55%) (rel. int. %): 164(26); 98(100).

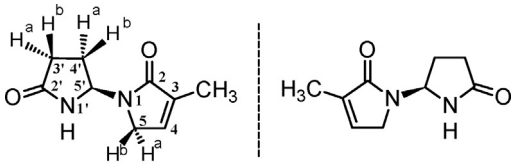

(±)-**4**

4.11. 3-Methyl-1-(3′-methyl-2′-oxopyrrolidin-5′-yl)-3-pyrrolin-2-one (**5**)

To a solution of 3-methyl-3-pyrrolin-2-one (**17**) (50.0 mg, 515 μmol) in THF (2 mL) 5-hydroxy-3-methylpyrrolidin-2-one (**19**) (60.0 mg, 521 μmol) and *p*-toluenesulfonic acid monohydrate (7.00 mg, 36.8 μmol) were added. The mixture was stirred at room temperature for 1 h, after which the mixture turned opaque. The solvent was removed under reduced pressure and the product was recrystallized using a mixture of hexane and ethyl acetate. The product was filtered and the crystals were dried by suction, giving the title compound **5** as a white crystalline solid (87.0 mg, 87%),

mp 168–172 °C (lit.: 172–174 °C) [11]; R_f (DCM:MeOH = 10:1) 0.52; ν_{max} (KBr) 3193, 3094, 2978, 1709, 1677, 1650, 1454, 1382, 1238, 1181 cm^{-1}; HRMS: M+H = 195.11283 (delta = 0.13 ppm; $C_{10}H_{15}O_2N_2$); HR-ESI-MS-MS (CID = 55%, rel. int. %): 178(54); 138(8); 98(100).

4.12. (3′R*,5′R*)-1-(3′-methyl-2′-oxo-5′-pyrrolidinyl)-3-methyl-3-pyrrolin-2-one (**5a**)

^{1}H NMR (500 MHz; acetone-d_6) δ (ppm) 1.14 (3H; d; J = 7.2 Hz; C(3′)-C$\underline{H}_3$); 1.78–1.79 (3H; m; C (3)-C$\underline{H}_3$); 2.14 (1H; ddd; J = 13.7, 9.5, 8.2 Hz; H^a-4′); 2.32 (1H; ddd; J = 13.7, 8.7, 1.5 Hz; H^b-4′); 2.64 (1H; ddq; J = 9.5, 8.7, 7.2 Hz; H-3′); 3.87–4.00 (2H; m; H_2-5); 5.69–5.73 (1H; m; H-5′); 6.85–6.87 (1H; m; H-4); 7.23 (1H; br; NH-1′); ^{13}C NMR (126 MHz; acetone-d_6) δ (ppm) 11.1 (C(3)-$\underline{C}H_3$); 16.6 (C(3′)-$\underline{C}H_3$); 35.1 (C-3′); 35.8 (C-4′); 46.7 (C-5); 60.3 (C-5′); 135.2 (C-3); 137.4 (C-4); 171.9 (C-2); 179.5 (C-2′); Lit. ^{1}H NMR [11]: 1.14 (3H; d; J = 7.1 Hz; C(3′)-C$\underline{H}_3$); 1.78 (3H; ddd; J = 2.0, 2.0, 1.8 Hz; C(3)-C$\underline{H}_3$); 2.13 (1H; ddd; J = 13.7, 9.5, 8.1 Hz; H^x-4′); 2.32 (1H; dddd; J = 13.7, 8.7, 1.9, 0.7 Hz; H^y-4′); 2.63 (1H; ddqd; J = 9.5, 8.7, 7.1, 0.3 Hz; H-3′); 3.90, 3.96 (2H; m; ^2J = 19.3 Hz, ^4J = 2.0 Hz (H-4), ^5J = 2.0 Hz (C (3)-C$\underline{H}_3$); H_2-5); 5.70 (1H; dddddd; J = 8.1, 1.9, 1.3, 0.6, 0.5, 0.5 Hz; H-5′); 6.85 (1H; ddqd; J = 2.0, 2.0, 1.8, 0.6 Hz; H-4); 7.12 (1H; br s; J = 1.3, 0.7, 0.3 Hz; NH-1′).

4.13. (3′S*,5′R*)-1-(3′-methyl-2′-oxo-5′-pyrrolidinyl)-3-methyl-3-pyrrolin-2-one (**5b**)

^{1}H NMR (500 MHz; acetone-d_6) δ (ppm) 1.18 (3H; d; J = 7.1 Hz; C(3′)-C$\underline{H}_3$); 1.73 (1H; ddd; J = 12.9, 9.4, 7.4 Hz; H^b-4′); 1.79–1.80 (3H; m; C(3)-C$\underline{H}_3$); 2.46–2.51 (1H; m; H-3′); 2.56–2.61 (1H; m; H^a-4′); 3.87–4.00 (2H; m; H_2-5); 5.80 (1H; ~t; J = 7.4 Hz; H-5′); 6.88–6.90 (1H; m; H-4); 7.08 (1H; br; NH-1′); ^{13}C NMR (126 MHz; acetone-d_6) δ (ppm) 11.1 (C(3)-$\underline{C}H_3$); 16.3 (C(3′)-$\underline{C}H_3$); 34.8 (C-4′); 36.5 (C-3′); 46.0 (C-5); 60.7 (C-5′); 135.2 (C-3); 137.8 (C-4); 172.4 (C-2); 178.4 (C-2′).

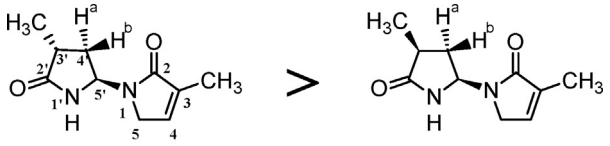

(±)-**5a** (±)-**5b**

diastereomeric ratio: ca. 85 : 15

4.14. 5-Hydroxy-3-methyl-1-(2′-oxopyrrolidin-5′-yl)-3-pyrrolin-2-one (**6**)

To a solution of jatropham **1** (90.0 mg, 796 μmol) in THF (5 mL) 5-ethoxypyrrolidin-2-one (**18**) (103 mg, 800 μmol) and *p*-toluenesulfonic acid monohydrate (10.0 mg, 52.6 μmol) were added. The mixture was stirred at room temperature for 1 h, after which a white crystalline solid precipitated. The solvent was removed under reduced pressure and the crude product was triturated in ethyl acetate. The suspension was cooled to 0–5 °C and the product was filtered. The crystals were washed with cold ethyl acetate and were dried by suction, giving the title compound **6** as a white crystalline solid (95.0 mg, 61%), mp 174–178 °C (lit.: 176–178 °C) [12]; R_f (DCM:MeOH = 10:1) 0.35; ν_{max} (KBr) 3209, 2998, 2977, 2924, 1718, 1695, 1661, 1460, 1417, 1381, 1296, 1281, 1238, 1091, 1079, 1031 cm^{-1}; HRMS: M+H = 197.09201 (delta = −0.30 ppm; $C_9H_{13}O_3N_2$); HR-ESI-MS-MS (CID = 35%, rel. int. %): 179(100).

4.15. (5S*,5′R*)-5-hydroxy-3-methyl-1-(2′-oxopyrrolidin-5′-yl)-3-pyrrolin-2-one (**6a**)

^{1}H NMR (800 MHz; acetone-d_6: methanol-d_4 = 1:1 (v/v)) δ (ppm) 1.82 (3H; m; C(3)-C$\underline{H}_3$); 2.30 (1H; ddd; J = 16.9, 10.3, 3.4 Hz; H^a-3′); 2.35 (1H; dddd; J = 13.9, 9.8, 3.4, 2.4 Hz; H^b-4′); 2.57 (1H; dddd; J = 13.9, 10.3, 8.7, 8.3 Hz; H^a-4′); 2.75 (1H; ddd; 16.9, 9.8, 8.3; H^b-3′); 5.51 (1H; dd; J = 8.7, 2.4 Hz; H-5′); 5.53–5.55 (1H; m; H-5); 6.67–6.68 (1H; m; H-5); Lit. ^{1}H NMR [12]: 1.83 (3H; dd; J = 1.8, 1.4 Hz; C(3)-C$\underline{H}_3$); 2.29 (1H; m; H^x-3); 2.34 (1H; m; H^x-4); 2.57 (1H; m; H^y-4); 2.75 (1H; m; H^y-3); 5.51 (1H; dd; J = 8.7, 2.4 Hz; H-5′); 5.53 (1H; dq; J = 1.8, 1.4 Hz; H-5); 6.68 (1H; dq; J = 1.8, 1.8 Hz; H-4); ^{13}C NMR (126 MHz; acetone-d_6: methanol-d_4 = 1:1 (v/v)) δ (ppm) 10.6 (C(3)-$\underline{C}H_3$); 26.2 (C-4′); 30.6 (C-3′); 63.7 (C-5′); 82.3 (C-5); 136.5 (C-3); 141.6 (C-4); 171.7 (C-2); 180.4 (C-2′).

4.16. (5R*,5′R*)-5-hydroxy-3-methyl-1-(2′-oxopyrrolidin-5′-yl)-3-pyrrolin-2-one (**6b**)

^{1}H NMR (800 MHz; acetone-d_6: methanol-d_4 = 1:1 (v/v)) δ (ppm) 1.83 (3H; m; C(3)-C$\underline{H}_3$); 2.27 (1H; ddd; J = 17.1, 10.2, 3.6 Hz; H^a-3′); 2.38 (1H; dddd; J = 13.6, 9.8, 3.5, 2.5 Hz; H^b-4′); 2.51 (1H; dddd; J = 13.6, 10.2, 8.5, 8.3 Hz; H^a-4′); 2.69 (1H; ddd; J = 17.1, 9.8, 8.3 Hz; H^b-3′); 5.47–5.49 (1H; m; H-5); 5.73 (1H; dd; J = 8.5, 2.5 Hz; H-5′); 6.68–6.69 (H-4). ^{13}C NMR (126 MHz; acetone-d_6: methanol-d_4 = 1:1 (v/v)) δ (ppm) 10.6 (C(3)-$\underline{C}H_3$); 27.1 (C-4′); 30.1 (C-3′); 63.5 (C-5′); 80.9 (C-5); 136.0 (C-3); 141.7 (C-4); 171.9 (C-2); 180.6 (C-2′).

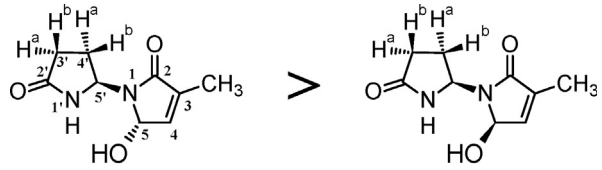

(±)-**6a** (±)-**6b**

diastereomeric ratio: ca. 79 : 21

4.17. 5-Hydroxy-3-methyl-1-(3′-methyl-2′-oxopyrrolidin-5′-yl)-3-pyrrolin-2-one (**7**)

To a solution of jatropham **1** (67.5 mg, 597 μmol) in THF (10 mL) 5-hydroxy-3-methylpyrrolidin-2-one (**19**) (69.0 mg, 599 μmol) and *p*-toluenesulfonic acid monohydrate (7.50 mg, 39.4 μmol) were added. The mixture was stirred at room temperature for 1 h, after which it turned opaque. The solvent was removed under reduced pressure and the crude product was purified by column chromatography (100 g silica) using DCM:MeOH (10:1) as the eluent. The fractions of the major product (R_f = 0.40) were combined and the solvent was evaporated, giving the title compound **7** as a white crystalline solid (54.0 mg, 43%), mp 162–164 °C (lit.: 169–171 °C) [11]; R_f (DCM:MeOH = 10:1) 0.40; ν_{max} (KBr) 3246, 3077, 2923, 1680, 1661, 1384, 1286, 1239, 1078 cm^{-1}; HRMS: M+H = 211.10758 (delta = −0.7 ppm; $C_{10}H_{15}O_3N_2$); HR-ESI-MS-MS (CID = 35%; rel. int. %): 193 (100).

*4.18. rel-(5S,3′R,5′R)-5-hydroxy-3-methyl-1-(3′-methyl-2′-oxopyrrolidin-5′-yl)-3-pyrrolin-2-one (**7a**)*

^{1}H NMR (800 MHz; acetone-d_6) δ (ppm) 1.133 (3H; d; J = 7.3 Hz; C(3′)-C$\underline{H}_3$); 1.77 (3H; m; C(3)-C$\underline{H}_3$); 2.11 (1H; ddd; J = 13.6, 8.9, 8.6 Hz; H^a-4′); 2.54 (1H; ddd; J = 13.6, 9.1, 1.2 Hz; H^b-4′); 2.92 (1H; ddq; 9.1, 8.9, 7.3 Hz; H-3′); 5.24 (1H; d; J = 10.0 Hz; C(5)-O$\underline{H}$); 5.45 (1H; ddd; J = 8.6, 1.4, 1.2 Hz; H-5′); 5.57–5.59 (1H; m; H-5); 6.62–6.65 (1H; m; H-4); 7.30 (1H; br; NH-1′); Lit. ^{1}H NMR [11]: 1.12 (3H; d; J = 7.2 Hz; C(3′)-C$\underline{H}_3$); 1.77 (3H; dd; J = 1.8, 1.3 Hz; C(3)-C$\underline{H}_3$); 2.10 (1H; ddd; J = 13.7, 9.5, 8.5 Hz; H^x-4′); 2.54 (1H; dddd; J = 13.7, 8.7, 1.4, 0.8 Hz; H^y-4′); 2.85 (1H; ddq; J = 9.5, 8.7, 7.2 Hz; H-3′); 4.83 (1H; d; J = 10.1 Hz; C(5)-O$\underline{H}$); 5.40 (1H; ddd; J = 8.5, 1.4, 1.4 Hz; H-5′); 5.54 (1H; ddq; J = 10.1, 1.8, 1.3 Hz; H-5); 6.20 (1H; qd; J = 1.8, 1.8 Hz; H-4); 6.86 (1H; br s; J = 1.4 Hz, 0.8 Hz; NH-1′); ^{13}C NMR (201 MHz; acetone-d_6) δ (ppm) 10.64 (C(3)-C$\underline{H}_3$); 16.5 (C(3′)-C$\underline{H}_3$); 35.12 (C-4′); 35.7 (C-3′); 60.9 (C-5′); 81.9 (C-5); 136.2 (C-3); 140.8 (C-4); 170.6 (C-2); 180.7 (C-2′).

*4.19. rel-(5R,3′R,5′R)-5-hydroxy-3-methyl-1-(3′-methyl-2′-oxopyrrolidin-5′-yl)-3-pyrrolin-2-one (**7b**)*

^{1}H NMR (800 MHz; acetone-d_6) δ (ppm) 1.127 (3H; d; J = 7.2 Hz; C(3′)-C$\underline{H}_3$); 1.77 (3H; m; C(3)-C$\underline{H}_3$); 2.07 (1H; ddd; J = 13.3, 9.2, 8.6 Hz; H^a-4′); 2.55 (1H; dddd; J = 13.3, 8.9, 1.2, 0.4 Hz; H^b-4′); 2.88 (1H; ddq; J = 9.2, 8.9, 7.3 Hz; H-3′); 5.22 (1H; d; J = 10.0 Hz; C(5)-O$\underline{H}$); 5.49–5.51 (1H; m; H-5); 5.62 (1H; ddd; J = 8.6, 1.4, 1.2 Hz; H-5′); 6.62–6.65 (1H; m; H-4); 7.38 (1H; br; NH-1′); ^{13}C NMR (201 MHz; acetone-d_6) δ (ppm) 10.63 (C(3)-C$\underline{H}_3$); 16.4 (C(3′)-C$\underline{H}_3$); 35.13 (C-3′); 36.2 (C-4′); 60.7 (C-5′); 80.5 (C-5); 135.8 (C-3); 141.1 (C-4); 170.9 (C-2); 181.0 (C-2′).

*4.20. rel-(5S,3′S,5′R)-5-hydroxy-3-methyl-1-(3′-methyl-2′-oxopyrrolidin-5′-yl)-3-pyrrolin-2-one (**7c**)*

^{1}H NMR partial assignment (800 MHz; acetone-d_6) δ (ppm) 1.22 (3H; d; J = 7.1 Hz; C(3′)-C$\underline{H}_3$); 1.77 (3H; m; C(3)-C$\underline{H}_3$); 2.17 (1H; ddd; J = 12.7, 9.1, 7.2 Hz; H^b-4′); 2.49–2.53 (1H; m; H-3′); 2.58 (1H; ddd; J = 12.7, 9.3, 7.6 Hz; H^a-4′); 5.36 (1H; d; J = 9.4 Hz; C(5)-O$\underline{H}$); 5.57 (1H; dd; J = 7.6, 7.2 Hz; H-5′); 5.62–5.65 (1H; m; H-5); 6.62–6.65 (1H; m; H-4); ^{13}C NMR partial assignment (201 MHz; acetone-d_6) δ (ppm) 15.9 (C(3′)-C$\underline{H}_3$); 33.8 (C-4′); 36.6 (C-3′); 61.68 (C-5′); 81.5 (C-5); 179.0 (C-2′).

*4.21. rel-(5R,3′S,5′R)-5-hydroxy-3-methyl-1-(3′-methyl-2′-oxopyrrolidin-5′-yl)-3-pyrrolin-2-one (**7d**)*

^{1}H NMR partial assignment (800 MHz; acetone-d_6) δ (ppm) 1.20 (3H; d; J = 6.9 Hz; C(3′)-C$\underline{H}_3$); 1.77 (3H; m; C(3)-C$\underline{H}_3$); 2.39 (1H; ddd; J = 12.4, 9.6, 7.4 Hz; H^b-4′); 2.49–2.53 (2H; m; H-3′, H^a-4′); 5.33 (1H; d; J = 9.6 Hz; C(5)-O$\underline{H}$); 5.63–5.66 (1H; m; H-5); 5.68 (1H; t; J = 7.4 Hz; H-5′); 6.62–6.65 (1H; m; H-4); ^{13}C NMR partial assignment (201 MHz; acetone-d_6) δ (ppm) 10.6 (C(3)-C$\underline{H}_3$); 16.0 (C(3′)-C$\underline{H}_3$); 34.2 (C-4′); 36.7 (C-3′); 61.68 (C-5′); 80.6 (C-5); 179.4 (C-2′).

*4.22. 5-Hydroxy-3-methyl-1-(3′-methyl-2′-oxo-3′-pyrrolin-5′-yl)-3-pyrrolin-2-one (**8**)*

To a solution of jatropham (**1**) (100 mg, 884 μmol) in THF (5 mL) *p*-toluenesulfonic acid monohydrate (11.0 mg, 57.8 μmol) were added. The mixture was stirred at room temperature for 1 h, after which a white crystalline solid precipitated. The mixture was evaporated under reduced pressure to ca. Half volume. The suspension was cooled to 0–5 °C and the product was filtered. The crystals were washed with cold THF and were dried by suction, giving the title compound **8** as a white crystalline solid (47.0 mg, 51%), mp 192–194 °C (lit.: 194–198 °C) [13]; R_f (DCM:MeOH = 10:1) 0.45; ν_{max} (KBr) 3326, 3222, 3073, 2920, 1706, 1678, 1661, 1645, 1402, 1291, 1098, 1075 cm^{-1}; HRMS: M+H = 209.09197 (delta = −0.47 ppm; $C_{10}H_{13}O_3N_2$); HR-ESI-MS-MS (CID = 35%, rel. int. %): 191(100); 163(1).

4.23. (5S,5′R*)-5-hydroxy-3-methyl-1-(3′-methyl-2′-oxo-3′-pyrrolin-5′-yl)-3-pyrrolin-2-one (**8a**)*

^{1}H NMR (500 MHz; methanol-d_4) δ (ppm) 1.85 (3H; dd; J = 1.7, 1.4 Hz; C(3)-C$\underline{H}_3$); 1.90 (3H; t; J = 1.7 Hz; C(3′)-C$\underline{H}_3$); 5.39–5.41 (1H; m; H-5); 5.95–5.97 (1H; m; H-5′); 6.63–6.65 (1H; m; H-4); 6.76–6.77 (1H; m; H-4′); Lit. ^{1}H NMR [13]: 1.85 (3H; dd; J = 1.7, 1.4 Hz; C(3)-C$\underline{H}_3$); 1.91 (3H; dd; J = 1.7, 1.7 Hz; C(3)-C$\underline{H}_3$); 5.40 (1H; dqd; J = 1.8, 1.4, 0.3 Hz; H-5); 5.96 (1H; dqdd; J = 2.0, 1.7, 0.4, 0.3 Hz; H-5′); 6.64 (1H; dqd; J = 1.8, 1.7, 0.4 Hz; H-4); 6.76 (1H; dq; J = 2.0, 1.7 Hz; H-4′); ^{13}C NMR (126 MHz; methanol-d_4) δ (ppm) 10.70, 10.76 (C(3)-C$\underline{H}_3$, C(3′)-C$\underline{H}_3$); 64.0 (C-5′); 82.5 (C-5); 136.3 (C-3); 139.0 (C-3′); 139.4 (C-4′); 142.4 (C-4); 172.6 (C-2); 175.5 (C-2′).

4.24. (5R,5′R*)-5-hydroxy-3-methyl-1-(3′-methyl-2′-oxo-3′-pyrrolin-5′-yl)-3-pyrrolin-2-one (**8b**)*

^{1}H NMR (500 MHz; methanol-d_4) δ (ppm) 1.86 (3H; dd; J = 1.7, 1.4 Hz; C(3)-C$\underline{H}_3$); 1.88 (3H; t; J = 1.7 Hz; C(3′)-C$\underline{H}_3$); 5.24–5.26 (1H; m; H-5); 6.10–6.12 (1H; m; H-5′); 6.66–6.68 (1H; m; H-4); 6.77–6.79 (1H; m; H-4′); ^{13}C NMR (126 MHz; methanol-d_4) δ (ppm) 10.67, 10.70 (C(3)-C$\underline{H}_3$, C(3′)-C$\underline{H}_3$); 63.3 (C-5′); 79.9 (C-5); 136.1 (C-3); 136.9 (C-3′); 141.7 (C-4′); 142.8 (C-4); 173.3 (C-2); 176.1 (C-2′).

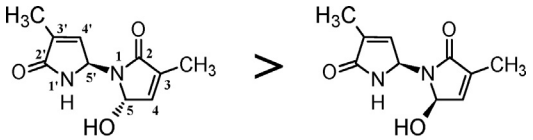

(±)-**8a** (±)-**8b**

*4.25. Lilaline [8-(3″-methyl-2″-oxopyrrolidin-5″-yl)kaempferol] (**14**)*

To a refluxing solution of kaempferol (**15**) (205 mg, 716 μmol) in nitromethane (10 mL) 5-hydroxy-3-methylpyrrolidin-2-one (**19**) (99.0 mg, 860 μmol) and *p*-toluenesulfonic acid monohydrate (15.0 mg, 78.9 μmol) were added. After 2 h yellow crystals

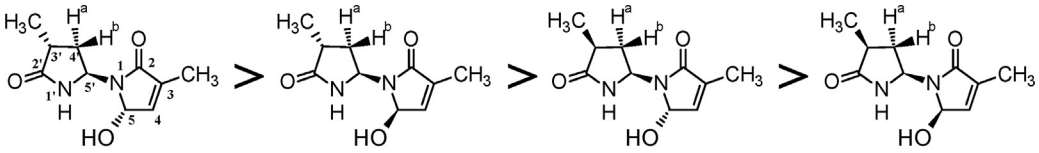

(±)-**7a** (±)-**7b** (±)-**7c** (±)-**7d**

diastereomeric ratio: ca. 53:35:7:5

precipitated. The reaction was monitored by TLC (DCM:MeOH = 10:1). After completion of the reaction, the mixture was cooled to 0 °C and the crystalline product was filtered. The crystals were washed with cold nitromethane and were dried under an infrared lamp. The crude product weighed 272 mg (99%), a 100 mg sample of which was purified by preparative HPLC to yield the pure C8 isomer **14** (the title compound) in the form of a yellow crystalline solid (83.0 mg, 82%), mp 245–248 °C (lit.: 247 °C) [17]; R_f (DCM:MeOH = 10:1) 0.38; ν_{max} (KBr) 3159, 2810, 2731, 2665, 1631, 1596, 1400, 1349 cm^{-1}; HRMS: M+H = 384.10803 (delta = 0.7 ppm; $C_{20}H_{18}O_7N$). HR-ESI-MS-MS (CID = 35%; rel. int. %): 367(100); 339(24).

4.26

(3″*S**,5″*R**)-8-(3″-Methyl-2″-oxopyrrolidin-5″-yl)kaempferol (*trans*-**14**): ^{1}H NMR (500 MHz; DMSO-d_6) δ (ppm) 1.13 (3H; d; J = 7.4 Hz; C(3″)-C$\underline{H}_3$); 1.99 (1H; ddd; J = 12.7, 8.8, 5.0 Hz; H^x-4″); 2.38 (1H; ddd; J = 12.7, 9.6, 5.9 Hz; H^y-4″); 2.54 (1H; dqd; J = 9.6, 7.4, 5.0 Hz; H-3″); 5.35 (1H; dd; J = 8.8; 5.9 Hz; H-5″); 6.26 (1H; s; H-6); 6.87–6.91 (2H; m; H-3′, H-5′); 7.62–7.72 (1H; br; NH-1″); 7.93–7.98 (2H; m; H-2′, H-6′);* ^{13}C NMR (126 MHz; DMSO-d_6) δ (ppm) 16.9 (C(3″)-$\underline{C}H_3$); 34.2 (C-4″); 36.2 (C-3″); 45.2 (C-5″); 98.8 (C-6); 101.9 (C-10); 106.2 (C-8); 115.4 (C-3′, C-5′); 121.7 (C-1′); 129.4 (C-2′, C-6′); 135.2 (C-3); 146.4 (C-2); 154.2 (C-9); 159.2 (C-4′); 159.4 (C-5); 165.0 (C-7); 175.6 (C-4); 179.3 (C-2″). Lit. ^{1}H NMR [17]: (300 MHz; CD_3OD) δ (ppm) 1.29 (3H; d; J = 7.4 Hz; C(3″)-C$\underline{H}_3$); 2.17 (1H; ddd; J = 12.9, 8.9, 4.9 Hz; H^x-4″); 2.57 (1H; ddd; J = 12.9, 9.7, 5.9 Hz, H^y-4″); 2.77 (1H; dqd; J = 9.7, 7.4, 4.9 Hz; H-3″); 5.56 (1H; dd; J = 8.9, 5.9 Hz; H-5″); 6.24 (1H; s; H-6); 6.91 (2H; d**; J = 9.0 Hz; H-3′, H-5′); 8.01 (2H; d**; J = 9.0 Hz; H-2′, H-6′); Lit. ^{13}C NMR [17]: (76 MHz; CD_3OD) δ (ppm) 17.5 (C(3″)-$\underline{C}H_3$); 35.9 (C-4″); 38.5 (C-3″); 48.1 (C-5″); 99.3 (C-6); 104.8 (C-10); 106.8 (C-8); 116.5 (C-3′, C-5′); 123.6 (C-1′); 130.8 (C-2′, C-6′); 137.1 (C-3); 148.5 (C-2); 155.9 (C-5); 160.7 (C-4′); 161.8 (C-9); 163.7 (C-7); 177.5 (C-4); 183.9 (C-2″).

4.27

(3″*S**,5″*S**)-8-(3″-Methyl-2″-oxopyrrolidin-5″-yl)kaempferol (*cis*-**14**): ^{1}H NMR (500 MHz; DMSO-d_6) δ (ppm) 1.05 (3H; d; J = 7.0 Hz; C(3″)-C$\underline{H}_3$); 1.94 (1H; ddd; J = 11.9, 11.5, 10.0 Hz; H^x-4″); 2.34 (1H; ddd; J = 11.9, 8.4, 6.6 Hz; H^y-4″); 2.48 (1H; ddq; J = 11.5, 8.4, 7.0 Hz; H-3″); 5.26 (1H; dd; J = 10.0, 6.6 Hz; H-5″); 6.25 (1H; s; H-6); 6.83–6.87 (2H; m; H-3′, H-5′); 7.79–7.87 (1H; br; NH-1″); 7.96–8.00 (2H; m; H-2′, H-6′);* ^{13}C NMR (126 MHz; DMSO-d_6) δ (ppm) 15.0 (C(3″)-$\underline{C}H_3$); 35.3 (C-4″); 36.6 (C-3″); 45.8 (C-5″); 98.6 (C-6); 102.1 (C-10); 104.5 (C-8); 115.3 (C-3′, C-5′); 121.7 (C-1′); 129.5 (C-2′, C-6′); 135.2 (C-3); 146.3 (C-2); 154.7 (C-9); 159.2 (C-4′); 159.5 (C-5); 165.2 (C-7); 175.5 (C-4); 178.2 (C-2″).

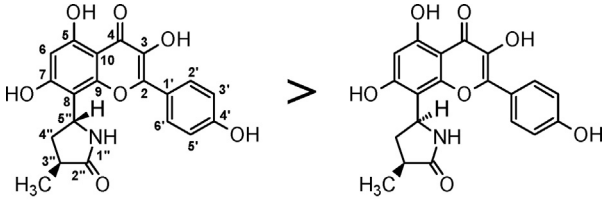

(±)-(3″*S**,5″*R**)-**14** > (±)-(3″*S**,5″*S**)-**14**

*The OH protons of the lilaline molecules were not observed as distinct resonances because the sample contained formic acid and water; the OH protons experienced fast chemical exchange and gave a common broad resonance at 4 ppm. **Actually, these resonances are AA'XX' multiplets, but were described as doublets in Ref. [17].

4.28. Modeling

MacroModel [43] was used for an initial conformational search and starting structure generation for the QM calculations. An OPLS3 force field [44] and water solvent were used (there is no methanol on the list of accessible solvents, but it was useable for starting structure generation.). The lowest energy structures in a 5 kcal/mol energy window were optimized at the B3LYP-D3/6-31+G** level [45–47] and the solution phase energy was determined using PBF methanol implicit solvation model [48,49]. In order to better sample the conformational space, the two lowest energy conformers having the hydrogen of the hydroxyl group rotated by about 180° were selected for a relaxed torsional scan around the C-5' – N-1 bond in all cases. The torsional scans were carried out at the B3LYP-D3/6-31+G** level in gas phase with a step size of 10° (except 8a and 8 b where a step size of 5° was applied) and the whole 0–360° interval was sampled. The effect of the solvent was taken into account in the course of single point calculations at the B3LYP-D3/6-31+G** level using PBF methanol solvation model. Further details are given in the SI. The Jaguar software was used for QM calculations [50]. Frequency calculations were carried out for the optimized global minima and no imaginary frequency was obtained. The effective proton-proton distances comparable to the distances derived from the NOE intensities were calculated with the following formula containing the Boltzmann factor and d^{-6} averaging [31].

$$d_{x,effective} = \left\{ \sum_i \left[\left(\frac{e^{-\frac{E_i}{RT}}}{\sum_j e^{-\frac{E_j}{RT}}} \right) \frac{1}{d_{x,i}^6} \right] \right\}^{-1/6}$$

where E_i and E_j is the calculated solution-phase energy of the conformer i and j.

Declaration of competing interest

The authors declare no conflict of interest.

Acknowledgments

The authors are grateful to Gedeon Richter Plc. for financial assistance. The authors wish to thank dr. Miklós Dékány (Gedeon Richter Plc., Spectroscopic Research Department, MS laboratory) and Barbara Herczeg (ComInnex, Inc.) for their contribution to the results presented in this manuscript.

Appendix A. Supplementary data

Supplementary data to this article can be found online at https://doi.org/10.1016/j.tet.2020.131827.

References

[1] (For information on lilies see:). (a) H.J. Elwes, A Monograph of the Genus Lilium, Taylor and Francis, London, 1880;
(b) H.B.D. Woodcock, W.T. Stearn, Lilies of the World: Their Cultivation and Classification, Country Life, London, 1950;
(c) P.M. Synge, Lilies: A Revision of Elwes' Monograph of the Genus Lilium and its Supplements, Universe Books, New York, 1980;
(d) E.A. McRae, Lilies: A Guide for Growers and Collectors, Timber Press, Oregon, 1998.
[2] (For more information on the medicinal aspects of lilies see:). (a) M. Grieve, A Modern Herbal, vols. 1–2, Dover Publications, New York, 1971;
(b) D. Brown, Encyclopedia of Herbs and Their Uses, Dorling Kindersley,

London, 1995;
(c) R. Chiej, Encyclopedia of Medicinal Plants (Macdonald Encyclopedias), MacDonald, London, 1984;
(d) N. Al-Bayati, J. Pharmaceut. Sci. Res. 10 (2018), 2014–2016;
(e) J. Patocka, Z. Biomed Navratilova, J. Sci. & Tech. Res. 18 (2019) 13859–13862;
(f) P. Wang, J. Li, F.A.K. Attia, W. Kang, J. Wei, Z. Liu, C. Li, Food Sci. Hum. Well. 8 (2019) 330–336;
(g) S. Momtaz, M. Dibaj, A. Abdollahi, G. Amin, R. Bahramsoltani, M. Abdollahi, P. Mahdaviani, A.H. Abdolghaffari, J. Med. Plants 19 (2020) 109–118;
(h) M. Zaccai, L. Yarmolinsky, B. Khalfin, A. Budovsky, J. Gorelick, A. Dahan, S. Ben-Shabat, Plants 9 (2020) 959.
[3] R.M. Wiedhopf, E.R. Trumbull, J.R. Cole, J. Pharmacol. Sci. 62 (1973) 1206–1207.
[4] K. Yakushijin, M. Kozuka, Y. Ito, R. Suzuki, H. Furukawa, Heterocycles 14 (1980) 1073–1076.
[5] K. Yakushijin, R. Suzuki, R. Hattori, H. Furukawa, Heterocycles 16 (1981) 1157–1160.
[6] T. Nagasaka, S. Esumi, N. Ozawa, Y. Kosugi, F. Hamaguchi, Heterocycles 16 (1981), 1987–1992.
[7] A. Vachálková, E. Eisenreichová, M. Haladová, P. Mučaji, B. Jožová, L. Novotný, Neoplasma 47 (2000) 313–318.
[8] G. Jovtchev, S. Gateva, A. Stankov, Environ. Toxicol. 31 (2016) 751–764.
[9] H. Shimomura, Y. Sashida, Y. Mimaki, Y. Minegishi, Phytochemistry 26 (1987) 582–583.
[10] E. Eisenreichová, M. Haladová, A. Bučková, K. Ubik, D. Uhrín, Chem. Pap. 45 (1991) 709–711.
[11] M. Haladová, E. Eisenreichová, A. Bučková, J. Tomko, D. Uhrín, Collect. Czech Chem. Commun. 53 (1988) 157–160.
[12] E. Eisenreichová, M. Haladová, A. Bučková, J. Tomko, D. Uhrín, K. Ubik, Phytochemistry 31 (1992) 1084–1085.
[13] M. Haladová, E. Eisenreichová, A. Bučková, J. Tomko, D. Uhrín, K. Ubik, Collect. Czech Chem. Commun. 56 (1991) 436–438.
[14] F. Pavelčík, Acta Crystallogr. C45 (1989) 956–957.
[15] K. Ori, Y. Mimaki, K. Mito, Y. Sashida, T. Nikaido, T. Ohmoto, A. Masuko, Phytochemistry 31 (1992) 2767–2775.
[16] T. Satou, Y. Mimaki, M. Kuroda, Y. Sashida, Y. Hatakeyama, Phytochemistry 41 (1996) 1225–1230.
[17] I. Mašterová, D. Uhrín, J. Tomko, Phytochemistry 26 (1987) 1844–1845.
[18] (a) E. Eisenreichová, I. Mašterová, A. Bučková, M. Haladová, J. Tomko, Českoslov. Farm. 34 (1985) 408–409;
(b) E. Eisenreichová, M. Haladová, P. Mučaji, D. Grančai, Acta Fac. Pharm. Univ. Comenianae 51 (2004) 27–37.
[19] A. Bučková, E. Eisenreichová, M. Haladová, D. Uhrín, J. Tomko, Phytochemistry 27 (1988) 1914–1915.
[20] (For our previous works in the field see:). (a) V. Ilkei, K. Faragó, Z. Sánta, M. Dékány, L. Hazai, C. Szántay Jr., C. Szántay, G. Kalaus, Int. J. Org Chem. 4 (2014) 309–313;
(b) V. Ilkei, P. Bana, F. Tóth, A. Palló, T. Holczbauer, M. Czugler, Z. Sánta, M. Dékány, Á. Szigetvári, L. Hazai, C. Szántay Jr., C. Szántay, G. Kalaus, Tetrahedron 71 (2015) 9579–9586;
(c) V. Ilkei, A. Spaits, A. Prechl, Á. Szigetvári, Z. Béni, M. Dékány, C. Szántay Jr., J. Müller, Á. Könczöl, Á. Szappanos, A. Mándi, S. Antus, A. Martins, A. Hunyadi, G.T. Balogh, G. Kalaus, H. Bölcskei, L. Hazai, T. Kurtán, Beilstein J. Org. Chem. 12 (2016) 2523–2534;
(d) V. Ilkei, A. Spaits, A. Prechl, J. Müller, Á. Könczöl, S. Lévai, E. Riethmüller, Á. Szigetvári, Z. Béni, M. Dékány, A. Martins, A. Hunyadi, S. Antus, C. Szántay Jr., G.T. Balogh, G. Kalaus, H. Bölcskei, L. Hazai, Tetrahedron 73 (2017) 1503–1510.
[21] (For reviews on the chemistry of N-acyliminium ions and the synthesis of their precursors see:). (a) W.N. Speckamp, H. Hiemstra, Tetrahedron 41 (1985) 4367–4416;
(b) W.N. Speckamp, M.J. Moolenaar, Tetrahedron 56 (2000) 3817–3856;
(c) C.M. Marson, ARKIVOC 1–16 (2001);
(d) B.E. Maryanoff, H. Zhang, J.H. Cohen, I.J. Turchi, C.A. Maryanoff, Chem. Rev. 104 (2004) 1431–1628;
(e) J. Royer, M. Bonin, L. Micouin, Chem. Rev. 104 (2004) 2311–2352;
(f) A. Yazici, S.G. Pyne, Synthesis (2009) 339–368;
(g) A. Yazici, S.G. Pyne, Synthesis (2009) 513–541.
[22] J.C. Hubert, J.B.P.A. Wijnberg, W.N. Speckamp, Tetrahedron 31 (1975) 1437–1441.
[23] B.L. Bray, P.H. Mathies, R. Naef, D.R. Solas, T.T. Tidwell, D.R. Artis, J.M. Muchowski, J. Org. Chem. 55 (1990) 6317–6328.
[24] I.M. Downie, M.J. Earle, H. Heaney, K.F. Shuhaibar, Tetrahedron 49 (1993) 4015–4034.
[25] D.O.A. Garrido, G. Buldain, M.I. Ojea, B. Frydman, J. Org. Chem. 53 (1988) 403–407.
[26] G.P. Gardini, V. Bocchi, Gazz. Chim. Ital. 102 (1972) 91–101.
[27] J. Bessho, Y. Shimotsu, S. Mizumoto, N. Mase, H. Yoda, K. Takabe, Heterocycles 63 (2004) 1013–1016.
[28] (a) N. Mase, T. Nishi, M. Hiyoshi, K. Ichihara, J. Bessho, H. Yoda, K. Takabe, J. Chem. Soc., Perkin Trans. 1 (2002) 707–709;
(b) N. Mase, T. Nishi, Y. Takamori, H. Yoda, K. Takabe, Tetrahedron: Asymmetry 10 (1999) 4469–4471.
[29] P. Kuehne, M. Hesse, Tetrahedron 49 (1993) 4575–4580.
[30] (For relevant studies on regioselective phenolic Mannich reactions see:). (a) M. Tramontini, L. Angiolini, Mannich Bases – Chemistry and Uses, CRC Press, Boca Raton, 1994, pp. 32–38;
(b) Y. Omura, Y. Taruno, Y. Irisa, M. Morimoto, H. Saimoto, Y. Shigemasa, Tetrahedron Lett. 42 (2001) 7273–7275.
[31] D. Neuhaus, M.P. Williamson, The Nuclear Overhauser Effect in Structural and Conformational Analysis, *second ed.*, Wiley, New York, 2000.
[32] S.G. Smith, J.M. Goodman, J. Org. Chem. 74 (2009) 4597–4607.
[33] N. Grimblat, M.M. Zanardi, A.M. Sarotti, J. Org. Chem. 80 (2015) 12526–12534.
[34] G. Tarazona, G. Benedit, R. Fernández, M. Pérez, J. Rodríguez, C. Jiménez, C. Cuevas, J. Nat. Prod. 81 (2018) 343–348.
[35] C.P. Butts, C.R. Jones, E.C. Towers, J.L. Flynn, L. Appleby, N. Barron, J. *Org. Biomol. Chem.* 9 (2011) 177–184.
[36] C.R. Jones, C.P. Butts, J.N. Harvey, Beilstein J. Org. Chem. 7 (2011) 145–150.
[37] Engineering ToolBox, Dynamic viscosity of common liquids, Accessed on 18 Oct 2019, https://www.engineeringtoolbox.com/absolute-viscosity-liquids-d_1259.html, 2008.
[38] S. Boros, Z. Gáspári, G. Batta, Annu. Rep. NMR Spectrosc. 94 (2018) 1–39.
[39] S.H. Mari, P.C. Varras, A. Wahab, I.M. Choudhary, M.G. Siskos, I.P. Gerothanassis, Molecules 24 (2019) 2290.
[40] L.B. Casabianca, Magn. Reson. Chem. 58 (2020) 611–624.
[41] R.E. Lancaster Jr., C.A. VanderWerf, J. Org. Chem. 23 (1958) 1208–1209.
[42] M. Hall, C. Stueckler, H. Ehammer, E. Pointner, G. Oberdorfer, K. Gruber, B. Hauer, R. Stuermer, W. Kroutil, P. Macheroux, K. Faber, Adv. Synth. Catal. 350 (2008) 411–418.
[43] Schrödinger Release 2018-2, MacroModel, Schrödinger, LLC, New York, NY, 2018.
[44] E. Harder, W. Damm, J. Maple, C. Wu, M. Reboul, J.Y. Xiang, L. Wang, D. Lupyan, M.K. Dahlgren, J.L. Knight, J.W. Kaus, D.S. Cerutti, G. Krilov, W.L. Jorgensen, R. Abel, R.A. Friesner, J. Chem. Theor. Comput. 12 (2016) 281–296.
[45] A.D. Becke, J. Chem. Phys. 98 (1993) 5648–5652.
[46] C. Lee, W. Yang, R.G. Parr, Phys. Rev. B 37 (1988) 785–789.
[47] S. Grimme, J. Antony, S. Ehrlich, H. Krieg, J. Chem. Phys. 132 (2010) 154104.
[48] D.J. Tannor, B. Marten, R. Murphy, R.A. Friesner, D. Sitkoff, A. Nicholls, M. Ringnalda, W.A. Goddard III, B. Honig, J. Am. Chem. Soc. 116 (1994) 11875–11882.
[49] B. Marten, K. Kim, C. Cortis, R.A. Friesner, R.B. Murphy, M.N. Ringnalda, D. Sitkoff, B. Honig, J. Phys. Chem. 100 (1996) 11775–11788.
[50] A.D. Bochevarov, E. Harder, T.F. Hughes, J.R. Greenwood, D.A. Braden, D.M. Philipp, D. Rinaldo, M.D. Halls, J. Zhang, R.A. Friesner, Int. J. Quant. Chem. 113 (2013) 2110–2142 (Schrödinger Release 2018-1: Jaguar, Schrödinger, LLC, New York, NY, 2018.).